EVALUATION OF RNA QUALITY FROM FORMALIN FIXED AND PARAFFIN EMBEDDED SAMPLES: APPLICATIONS AND LIMITATIONS

by

XIAO ZHANG

A thesis submitted to the Department of Pathology and Molecular Medicine

in conformity with the requirements for

the degree of Master of Science

Queen's University

Kingston, Ontario, Canada

(September, 2008)

Abstract

RNA molecules isolated from FFPE samples are highly fragmented and modified, and generally deemed unsuitable for downstream gene expression profiling. With the development of molecular biology, there has been growing interest in profiling archival FFPE samples. Successful profiling of transcripts from FFPE samples would greatly expand tissue sources for large scale gene expression studies; also it would pave the way for future applications on the type of tissue readily available in the clinical setting. So far, there is a lack of systemic studies evaluating the quality of RNA isolated from routinely processed FFPE samples, and it has remained difficult to assess how well FFPE-derived RNA mirrors the status of RNA isolated before fixation. In this project, the similarity of miRNA and mRNA profiles between matched frozen and FFPE lymphoid hyperplasia tissues (N=7 for miRNA comparison, N=4 for mRNA comparison) were evaluated. We found consistently good correlation (mean of Pearson coefficient=0.939, mean of Spearman coefficient=0.905, mean of Kendall tau=0.744) between matched frozen and FFPE-derived miRNA profiles, suggesting FFPE samples may retain miRNA expression information quite well. This has major positive implications for research using FFPE samples, as miRNA profiling becomes more prominent in bioprofiling studies. On the contrary, mRNA isolated from FFPE samples showed less correlation (Spearman coefficient less than 0.75) with its frozen counterpart on the Agilent microarray platform. With a post extraction heat treatment aimed at reversing base modifications and cross linking structures, obvious global mRNA quality improvement was observed in cases where samples appeared to be heavily cross linked, but was less effective and even

detrimental in cases where cross linking was less prominent. This research suggests that the extent of cross linking may be critical in terms of determining whether a particular FFPE tissue will become a useful source of mRNA for global profiling studies

Acknowledgements

I would like to express my gratitude to all who gave me the possibility to complete this thesis. First and foremost, I would like to thank my supervisor Dr. Harriet Feilotter for giving me the opportunity to enroll in this program. Regardless of my long time absence from school study and limited lab experience, she took me under her supervision without hesitation. Her patience and encouragement guided me through numerous difficulties, making past two years a unique and pleasant Canadian learning experience in my life.

I also wish to express my sincerer thanks to Dr David LeBrun, Dr Scott Davey, Dr Victor Tron, Dr Tom Radcliffe for their detailed and constructive comments and support along the progress of this project.

Thanks to members in Dr Feilotter's lab, both past and present, Dr. Kristine Roland, Natasha Gallo, Yuhui Xu, Jim Gore, Hong Guo, Dr. Ashish Rajput, Dr. Alanna Church, Chris Chuyow and staff in Dr Tron's lab Kathleen Felton, Cindy Lentz, Jay Chen for their technical assistant and moral support. Especially to Jim and Hong, their mentorship in the early stage of my study makes me feel at home in the lab.

Especially, I would like to give special thanks to my family members, whose love supported me to complete this work.

Table of Contents

List of Figures

List of Tables

.

List of Abbreviations

BCR-ABL	breakpoint cluster region-Abelson murine leukemia viral oncogene
cDNA	complementary DNA
CEC	capping enzyme complex
CML	chronic myelogenous leukemia
Ct	threshold cycle
CUP	cancer of unknown primary origin
dAMP	deoxyadenosine
DASL	cDNA-mediated Annealing, Selection, Extension, and Ligation
FFPE	formalin fixed and paraffin embedded
FNA	fine needle aspiration
HIV	human immunodeficiency virus
HPLC	high performance liquid chromatography
IHC	immunohistochemistry
LNA	locked nucleic acid
miRNA	microRNA
mRNA	messenger RNA
OCT	optimal cutting temperature freezing medium
Pre-miRNA	precursor microRNA
Pri-miRNA	primary microRNA
qRT-PCR	quantitative reverse transcription polymerase chain reaction
RAKE	RNA primed, array based Klenow enzyme
RIN	RNA integrity number
RISC	RNA induced silencing complex
rRNA	ribosomal RNA
RT	reverse transcription
RT-PCR	reverse transcription polymerase chain reaction
SAGE	tag based serial analysis of gene expression
tRNA	transfer RNA
UTR	untranslated region

CHAPTER 1 General Introduction

1.1   Transcriptional level research

At the molecular level, all biological events in a cell are primarily controlled by DNAs, RNAs, proteins and metabolites, which interact with each other in a network. The network components and functional relationship between biomolecules vary over time and space. The genome contains the complete set of genes. These are sources of information which is context independent; i.e., most cells contain the same genome regardless of the type of cell, stage of development or environmental conditions. The transcription of genes, into either protein coding or non coding RNA, is context dependent, varies according to cell type and functional state of the cell. For example, specific gene expression patterns have been demonstrated in various physiological situations, such as cell division, proliferation, differentiation and apoptosis. Conversely, abnormal gene expression profiles have been shown in a vast array of diseases [1] [2] [3] [4] [5] [6]. Thus transcriptional level research provides information on gene expression status specific for a given biological process [7].

The completion of the human genome-sequencing project, together with major technical breakthroughs, has provided opportunities to carry out gene expression analysis in a multidimensional manner. Such broad transcriptional studies, coupled with DNA and protein level studies, have greatly advanced the uncovering of molecular mechanisms of disease, leading to discoveries of novel diagnostic, prognostic and predictive markers and to more specific targeted therapies [8] [9] [10] [11]. For example, LeBrun et al have developed an expression based prognostic predictor for non Hodgkin lymphoma [12].

300 candidate genes capable of predicting five year survival were identified by correlating gene expression profiles to survival information in 41 cases of follicular lymphoma. Similar approaches have been applied to other tumors including breast cancer, ovarian cancer, prostate cancer, melanomas and lung cancer with promising results [13] [14] [15] [16] [17]. For instance, gene expression profiling of node negative breast cancer samples generated a 70- gene signature to predict risks of metastasis, which has led to the clinical application of the first microarray based cancer predictive test (MammaPrint) [18] [19]. Compared to previous clinicopathological risk assessment strategies such as Europe St.Gallen and USA NIH consensus guidelines, MammaPrint provides more accurate prediction of metastasis to guide adjuvant therapy [19] [20]. It has been shown that around one third of patients would be exempted from unnecessary adjuvant therapy following MammaPrint predication. On the other hand, MammaPrint is almost as efficient as previous assessment strategies in categorizing high risk patients for more radical adjuvant therapy. It is obvious that application of MammaPrint greatly benefits patients by providing adjuvant therapy more tailored to the biology and severity of their disease and alleviates financial burden on health care system by cutting back unnecessary overtreatment.

Messenger RNAs (mRNAs) (1%-3% of the total RNA) and microRNAs (miRNAs) (less than 1% of the total RNA) are two major subjects in transcriptional level research. In eukaryotes, protein coding mRNA is synthesized by RNA polymerase II in the nucleus. Soon after initiation of transcription, nuclear Capping Enzyme Complex (CEC) adds nascent mRNA transcript with a 7-methylguanosine, which protects transcript from nuclease attack. As the polymerase moves from 5' to 3' along the gene, splicing factors

remove introns. Upon reaching the end of a gene, transcription is terminated and polyadenylation tail is added to the nascent mRNA transcript cleaved from polymerase. Mature mRNA is then transported into cytoplasm through the nuclear pore and serves as an intermediate template to guide protein synthesis [21].

miRNAs are a class of non protein coding small RNA (18~24 nt). The primary transcript for a miRNA (pri-miRNA, hundreds to thousands nucleotides long) is synthesized by polymerase II, which is further processed in the nucleus by the RNase III Drosha and its cofactor Pasha to yield 60-110 base pair, hairpin precursor miRNA (pre-miRNA). Pre-miRNAs are then transported by nuclear export factor Exportin-5 into the cytoplasm [22], where they are processed by Dicer, another multi-domain RNase III-type enzyme to generate a sequence-specific, single stranded mature miRNA molecule (~18-24nt) [23]. The resulting mature miRNA is then incorporated into a ribonucleoprotein complex called RNA-induced silencing complex (RISC), repressing gene expression at the post transcriptional level by binding 3' untranslated regions (3'UTR) of specific mRNA molecules based on sequence homology, leading to mRNA translational repression [23]. Repressed mRNAs are relocated to specific intracellular organelles called processing bodies for storage [24] [25]. A given mRNA often has multiple miRNA target sites, a property that makes it possible for a limited number of miRNAs to regulate a large number of mRNAs. Computational models have estimated 500-1000 miRNAs may be present in higher eukaryotes, and up to 30% of protein coding genes are estimated to be regulated by miRNAs [26].

Gene expression is highly dynamic and context dependant, and the levels of an individual mRNA/miRNA can vary greatly from cell to cell and time to time [27]. This is achieved

by highly regulated gene transcription initiation and quick transcript degradation. In eukaryotes, gene expression is initiated by transcription factors which bind to regulatory sequences located upstream of sites where the transcription begins [28]. The activities of these transcription factors are controlled by a variety of regulatory pathways. For example, transcription factors that regulate cell cycle related genes are controlled by cell cycle signals. After gene expression initiation, activated transcription factors are quickly deactivated by the ubiquitin protease system. On the other hand, most mRNAs/miRNAs are designed to be ephemeral molecules, having a half life of minutes to hours [29] [21] [30] [31]. Thus sample handling techniques to "freeze" transcript status for a given biological situation and precise gene expression profiling of those samples are key for obtaining biological meaningful data [7] [31].

1.2 Gene expression analysis platforms- quantitative reverse transcription polymerase chain reaction (qRT-PCR) and gene expression microarray

Various platforms have been developed to measure expression levels of genes of interest, including Northern hybridization, RNase protection assay, subtractive hybridization, and tag based serial analysis of gene expression (SAGE) [32] [33] [34]. Recently, more robust high throughput techniques such as quantitative reverse transcription polymerase chain reaction (qRT-PCR) and gene expression microarray have become mainstream quantification methods [35] [36].

Quantitative PCR is a technique based on PCR to amplify and quantify a targeted molecule, the core technology of which relies on the cyclical detection of the fluorescence produced by a reporter molecule that is proportional to product accumulated. qPCR is frequently coupled with a reverse transcription (RT) reaction to

quantify cDNA derived from RNA, a technique known as qRT-PCR. Compared to previous RNA quantification methods, qRT-PCR has several advantages: 1) the qPCR instrumentation measures the fluorescence at each PCR cycle as the amplification progresses. This allows accurate and reproducible quantification of cDNA based on the fluorescence signal during the exponential phase of amplification. 2) Post PCR gel electrophoresis, which is time consuming and not precise in quantification, is not necessary. 3) Using amplicon specific probes attached with different fluorescent chemistry, multiple targets can be measured in the same reaction. Currently, qRT-PCR has been applied widely in the clinical setting for various purposes. For example, in chronic myelogenous leukemia (CML), BCR-ABL fusion gene products in blood or bone marrow are measured using this technique to monitor treatment response and predicate the likelihood of relapse [37]. Likewise, qRT-PCR has been used to monitor viral load in human immunodeficiency virus (HIV) or hepatitis C virus infected patients [38] [39].

Gene expression microarray is a technique that investigates expression levels of multiple genes by hybridizing labeled RNA to gene specific probes fixed on a solid surface. Several different microarray platforms are available for gene expression analysis, including cDNA arrays, oligonucleotide arrays. Current technology has allowed us to measure expression levels of all genes known on a single array using RNA isolated from just a few cells. Taking the advantage of parallel gene expression measurement of this technique, expression profiling have been applied for various purposes such as: 1) to find expressed genes in a given sample or experimental condition, 2) to find differentially expressed genes between two samples or experimental conditions, 3) to find gene expression signatures with respect to particular conditions or classes of samples. In the

past decade, huge amounts of gene expression data have been generated by microarray experiments. With emerging novel data analysis tools, more information regarding the complex network of gene expression has been revealed with potential for future clinical application. For example, expression profiling has discovered gene signatures to identify the origin of cancer of unknown primary origin (CUP), a task which can't be fulfilled by conventional clinicopathological methods [40]. On the other hand, the technical variations introduced by sample heterogeneity, microarray platform variations and different statistical analyses employed by different groups pose huge challenges with respect to results comparison and validation, a problem that needs to be tackled by standardization of experiment design and analysis approaches.

Currently, qRT-PCR and gene expression microarray are often used in a serial fashion. While high throughput DNA microarrays lack the quantitative accuracy of qRT-PCR, it takes about the same time to measure the gene expression of a few dozen genes via qRT-PCR as it would to measure an entire genome on a microarray platform. So it often makes sense to perform gene expression microarray analysis experiments to identify candidate genes, then perform qRT-PCR on selected candidate genes to validate the microarray results.

1.3 Fresh or snap frozen sample preferred yet limited for RNA quantification

Regardless of the RNA quantification platform used, fresh or snap frozen samples are acknowledged to be the best source for intact RNA and subsequent accurate gene expression results. However, collecting fresh or frozen human solid tissues for gene expression studies proves difficult because formalin fixation and paraffin embedding (FFPE) is routinely performed in clinics to preserve samples for histological examination.

As a result, small samples, such as biopsies from fine needle aspiration (FNA) procedures, often only exist in FFPE format. Even when extra samples are available, it is more demanding, both logistically and administratively, to collect fresh or frozen samples for possible downstream gene expression studies. Consequently, fresh or snap frozen solid tissues are only available in certain well defined situations in large pathology laboratories when specific molecular research is planned [29]. Although many institutions are now building frozen tissue banks to meet increasing demands for molecular assays, few are at the stage to permit large scale genetic analyses or to have sufficiently long term follow up information to yield meaningful clinical data [41]. Therefore, tissue source becomes a bottleneck for large scale gene expression studies, which is especially relevant in cancer research targeting solid tumor types. On the other hand, FFPE-derived RNAs are generally deemed unsuitable for gene expression profiling because RNA molecules are highly fragmented and modified, and it remains unclear how well FFPE sample-derived RNA mirrors the status before fixation.

1.4 FFPE sample abundant yet RNA compromised

1.4.1 Formalin a widely used fixative to prepare tissues

Formalin is a saturated aqueous solution containing 37% formaldehyde (by weight) or 40% formaldehyde (by volume). Since its serendipitous discovery as a fixative in 1893, 10% formalin soon replaced alcohol as the most popular fixative for histological processing, because formalin preserves cellular structures with only marginal shrinkage and distortion of tissue, a property favored by pathologists [42]. To date, however, the mechanism of formalin fixation remains elusive in spite of its wide usage. It is suggested that formaldehyde, a reactive electrophilic reagent, cross links functional groups of

macromolecules, including proteins, nucleic acid, glycoproteins and polysaccharides. These intra-molecular and inter-molecular cross links alter physical characteristics of tissues, leading to fixation of the tissue.

1.4.2 Vast FFPE sample archive established

In today's medical practice, histological examination remains an indispensable tool to assist clinical decision making, such as diagnosis and choosing proper therapeutic regime. As a result, FFPE processing is a routine tissue preparation method performed on solid tissues, including most tumors. Vast archives of formalin fixed and paraffin embedded samples have been accumulated in the last century. It is estimated that there are more than one billion archival FFPE samples throughout the world [41]. Moreover, detailed histological annotation and long term follow up information are readily available from archival FFPE samples, which are valuable sources for large scale retrospective studies [29].

The importance of this huge tissue archive can not be underestimated. In addition to traditional histological examination, these FFPE samples are readily available for molecular investigation as new technologies develop at a remarkable speed. The value of these FFPE samples has been proven by the development of many immunohistochemical assays now routinely used as diagnostic procedures. Similarly, techniques for extraction and analysis of nucleic acid from FFPE samples have been optimized allowing various molecular assays to be performed on archival FFPE samples.

1.4.3 RNA fragmentation and modification during FFPE processing

Considering the widespread use of FFPE processing in clinics, it is a bit surprising that there are few circumstances under which a set of standardized guidelines for preparing FFPE samples has been employed. Although all protocols include major steps of formalin fixation, gradient ethanol dehydration, xylene clearing and paraffin embedding, how each procedure is performed may vary from sample to sample. Thus, it is difficult to evaluate the impact of each step on RNA molecules by studying FFPE samples processed in an uncontrolled manner. Recently, several studies have been carried out on in-lab made FFPE samples, showing how mRNA is compromised at individual steps of FFPE processing, which are detailed in the following section. It is speculated that miRNAs might be affected by FFPE processing in a similar manner; however, there have been no systematic studies performed to this date.

1.4.3.1 RNA fragmentation before fixation

Warm ischemia and/or tissue hypoxia after sample dissection has been demonstrated to trigger RNA fragmentation from both 5' and 3' directions, a process that continues until RNases are completely deactivated by formalin. However, the detailed mechanism of RNase release is not clear. The RNA loss is presumably greatest in tissues harboring high levels of endogenous RNases, such as pancreas, gall bladder and liver.

Previously, most researchers assumed that a delay of hours prior to complete tissue fixation would lead to complete degradation of most labile RNAs, making gene expression profiling almost impossible from samples with delayed fixation. However, recent systematic studies on a qRT-PCR platform have suggested this assumption might not be totally true. By experimenting on RNase rich liver tissue, Godfrey and his group found that a delay of up to 12 hours before formalin fixation did not significantly reduce
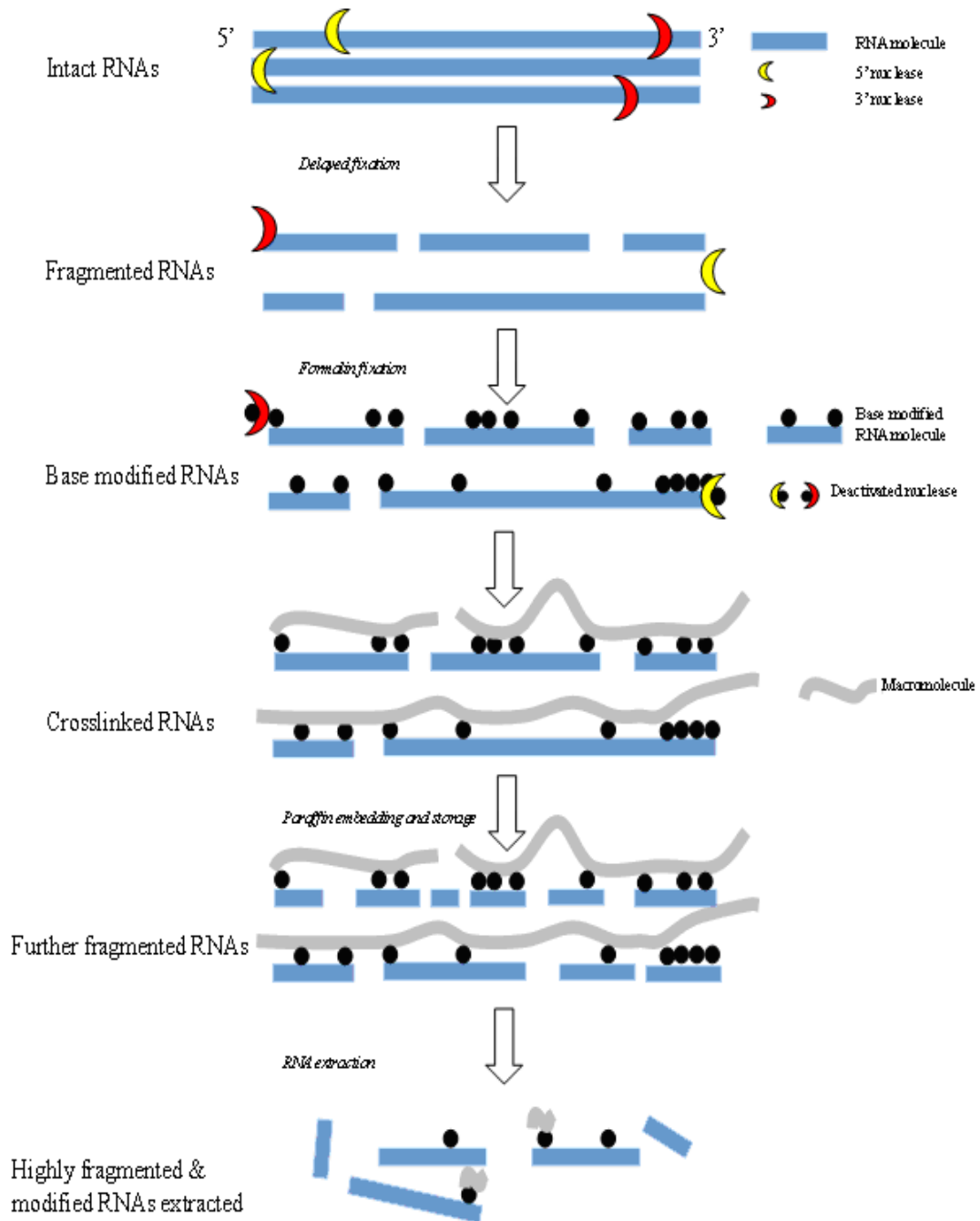
Figure 1-1 How the RNA molecule is compromised during FFPE processing: During a delayed fixation period, RNA is fragmented by endonucleases from 3' and 5' directions. Formalin fixation then adds hydroxymethyl groups to nucleotides, which further cross link with macromolecules to form a matrix complex. RNA continues to fragment during storage.

expression of *c-myc*, which has a reported half life as short as 10 minutes [43]. In another study, it has been shown that most degradation of RNAs occurs mainly within the first two hours after sample excision and reaches a plateau at more than 50% of original levels [44]. These observations are probably due to the following reasons: 1) *In vivo*, the steady state level of RNA is controlled by both transcription and degradation rates. Transcription may still occur due to residual metabolism after sample dissection, thus the total amount of RNA may decrease at a slower rate than expected based simply on half life estimation. It is worth noting that transcription rates of genes related to the stress response may be accelerated greatly due to hypoxia, depletion of nutrients imposed by ligation and excision, offsetting RNA fragmentation effects due to fixation delay. As a result, expression levels of those genes may not decrease that much compared with other genes. 2) Intact cell compartment and spatial hindrance by proteins may delay RNA degradation by RNases. 3) RNA may be fragmented, but still detectable on qRT-PCR platform using primers targeting short amplicons.

With the exception of small biopsies such as FNAs, formalin penetration into the sample is a time consuming step. Penetration rates decrease with depth, starting around 1mm per hour on the surface and taking about 8 hours to penetrate a 5mm sample. To avoid RNA degradation near the core of the thick sample, it is recommended that samples thickness should be around or below 5mm [44], although this recommendation is not routinely adhered to.

Reducing time delay and fixing small samples would effectively minimize RNA fragmentation before fixation. However, in reality, since these two factors have almost negligible effects on preservation of morphological features required for histological

assessment, it isn't uncommon in a clinical setting to see a fixation delay up to 12 hours and big chunks of samples fixed as a whole.

1.4.3.2 Base modification and cross linking during formalin fixation

Only a few papers have addressed the mechanism of the reaction between formalin and RNA. It is now believed that multiple reactions occur during the formalin fixation process.

1) Addition of hydroxymethyl(methylol) CH_2-OH groups to the nitrogen atom of the nucleic acid bases. Both exocyclic and endocyclic amino groups may react with formaldehyde. Equilibrium constants of the base modification reactions of the four RNA bases ranks as A>C>G>>U, suggesting adenine is most easily modified by formalin followed by cytidine, guanine, and uracil. Masuda [45] et al confirmed this affinity difference in 1999 by measuring the increased molecular weight of synthetic octamers of ribonucleotides under conditions simulating formalin fixation. They found at the end of a 16 hour formalin fixation, methylol groups were added to 39.2% of adenines, 32.9% of cytidines, 7.1% of guanines and 3.8% of uracils. Extending formalin fixation time to 7 days has been demonstrated to further increase bases modification percentages to 62.1%, 48.8%, 9.5%, 4.0% for octamers of adenine, cytidine, guanine and uracile respectively.

2) Slower electrophilic attack of the N-methylol group on an amino base to form a methylene bridge [45]. In the case of RNA, this reaction can cause cross linking between a RNA molecule and a protein molecule or other nucleic acids in cytoplasm. Although there is no doubt the cross linking reaction does occur during FFPE processing, it is still unclear how it occurs. Recently it has been suggested that cross linking may be initiated by ethanol dehydration step rather than by formalin itself as has been commonly

assumed. In one study, no cross linking products were detected by sensitive high-performance liquid chromatography (HPLC) methods even after incubating d-AMPs with formalin for up to 3 days. The authors suggested that it is the anhydrous conditions following dehydration in 100% ethanol that transforms N-methylol group (-NHCH2OH) into Schiff bases (-N=CH2), which readily react with neighboring amino groups by cross linking [46]. However because no such study was conducted using poly nucleotide substitutes, further investigations are needed to elucidate how cross linking happens.

3) Hydrolysis of N-glycosylic bonds and generation of apurinic and apyrimidinic sites. Depurination and depyrimidination are spontaneous alterations that occur to DNA under physiological conditions. On the contrary, abasic sites in RNA are rare because of the greater stability of the RNA sugar ring [47]. However, the stability of N-glycosylic bonds are greatly affected by chemical modifications added to RNA bases, leading to depurination and depyrimidination. It has been shown that depurination occurs as much as 500 times faster than depyrimidination with cleavage rates differing for the bases as guanosine>adenosine >>cytidine=uradine [47]. The cleavage increases at low pH and high temperatures. A 1- 3% base depurination has been revealed in formalin-fixed ethanol-dehydrated 2'-deoxyadenosine 5'-monophosphate (dAMP) [46]. Considering the fact that N-glycosylic bonds of 2' deoxyribosyl derivatives are hydrolyzed 100-1000 times faster compared to corresponding ribosyl derivatives and N-glycosylic bonds are more stable in polynucleosides than monnucleosides, the cleavage may happen to less than 0.04% of RNA bases [47]. Although possibility of depurination and depyrimidination is comparatively small, however, once it occurs, it impairs the association of enzymes and template in downstream molecular assays.

4) Slow hydrolysis of phosphodiester bonds cleaving RNA molecule into polynucleotides has also been reported, particularly during extended formalin fixation [48].

1.4.3.3 Fixation time and RNA quality

The duration of formalin fixation is another critical factor affecting RNA quality for downstream gene expression assays. A fixation time of 8~16 hours has been shown to produce a maximal length amplicon of 750bp using an RT-PCR platform [48][49]. In another study, RNA isolated from sample fixed overnight was shown to support the production of up to 800bp amplicons following RT-PCR, while only 400-600bp amplicons could be generated using RNA isolated from a sample fixed 72 hour. [50] [51]. Why a longer fixation time has negative effects on amplicon length assays still remains unclear. Some have suggested RNA fragmentation over extended fixation times [48], while other studies indicated that increased level of base modification and cross linking might be responsible for inferior performance on RT-PCR platform [45]. A recommended protocol is to have a formalin incubation time up to a maximum of 24 hours for regularly sized samples and shorter fixation times for smaller core or needle biopsies. Overfixed samples, such as those fixed over weekend or samples obtained in mail-in biopsy services, should be avoided for gene expression assays [51].

1.4.4.4 Storage conditions and RNA quality

FFPE samples are normally archived at room temperature. It has long been known that RNA fragmentation proceeds gradually over storage time. What causes the slow fragmentation remains unclear, however, it is unlikely due to enzymatic degradation as all endogenous RNases are fully deactivated and it is difficult for exogenous RNases to penetrate into paraffin blocks and degrade RNA molecules in a dehydrated situation.

Physical shear force may be a more plausible answer for this slow fragmentation. Recently, storage temperatures were demonstrated to have a profound influence on the extent of RNA fragmentation, with higher storage temperatures leading to faster RNA degradation [50]. RNA isolated from one year old FFPE samples may still have intact ribosomal RNA peaks on electrophoregram if harvested tissue was immediately processed and stored at 4° C, and up to 700 bp amplicons can be generated on RT-PCR platforms from the same RNA source. Conversely, when the same sample was stored at room temperature, ribosomal RNA peaks gradually disappeared over one year period and only 400 bp amplicon could be generated at the end of 12 months [50]. Exposing sliced FFPE samples sections to light and air has also been shown to negatively affect RNA quality [50]. This affect can be lessened by discarding the first several sections near the surface of FFPE sample block, which is always suggested in RNA extraction protocols.

1.5 RNA extraction from FFPE samples

RNA is readily extracted from fresh or frozen samples by homogenizing cells and then purifying RNA using a guanidinium thiocyanate-caesium chloride gradient or a column based procedure. These methods produce RNA with reasonable yield and quality for downstream molecular experiments. However, extraction of RNA from FFPE samples is more problematic. When the same RNA isolation protocols used for frozen samples were applied to FFPE samples, most of them failed to isolate enough RNA for downstream assays [52]. It has been demonstrated that breaking cells by homogenization is not enough to release RNA molecules into the extraction buffer [52].

To solve this problem, a number of procedures, such as heat treatment and sonication, have been tried to facilitate RNA release with varying success. [53] [54]. To date, the

most successful method to recover RNA from a FFPE sample includes digesting samples with proteinase K before RNA purification. Crosslinked proteins within fixed samples are readily dissolved in proteinase K solution, releasing RNA into extraction buffer [55]. Several commercially available RNA extraction kits based on this principle have been marketed. The yield may vary from kit to kit, but normally several micrograms of total RNA can be isolated from several 10 μm sections of most FFPE samples, which is enough for most downstream molecular assays. Unfortunately, RNA isolated using this method remains highly modified and fragmented. The average size of the fragmented RNA isolated from a FFPE sample is about 200 nucleotides as estimated from formaldehyde-agarose gel eletrophoresis [55].

1.6 Heat treatment and RNA quality improvement

A heat treatment was used to increase the signal strength from immunohisto-chemistry (IHC) assays done on FFPE samples in 1991 [56]. The suggested mechanism is that the heat breaks the epitope cross linking caused by formalin. Recently, it was realized the same cross linking mechanisms apply when formalin reacts with RNA molecules, and it was suggested that heat treatment of RNA extracted from FFPE samples may reverse the base modification and cross linking, making treated RNA a better template for cDNA synthesis. Several groups have demonstrated that heating RNA isolated from FFPE samples before reverse-transcription polymerase chain reaction (RT-PCR) results in increased amplicon size [45]. Previous studies have suggested that heating temperature, time, and pH of the buffer are all important factors in the heat treatment. However, no consensus has been reached in terms of optimal conditions to treat RNA [45] [53] [57].

1.7 Utilizing FFPE sample-derived RNA

1.7.1 Successful application

Since the first successful RNA extraction from FFPE sample in 1988 [58], there have been attempts to use this material in various molecular experiments because large numbers of samples with clinical outcome data can be rapidly acquired and analyzed.

So far, the application of FFPE sample-derived RNA has been successful in RT-PCR based assays to identify the presence of certain templates [59] [60]. In these assays, a less than 200bp amplicon is targeted to cope with RNA fragmentation. The success rate drops dramatically for amplicon above 200bp [52]. Considering the fact that the poly A tails of mRNA from FFPE samples are highly degraded and modified, random priming or gene specific priming is used to ensure successful cDNA generation. In addition, an in situ RT-PCR technique has been successfully applied on FFPE samples to show the localization of gene expression [61].

1.7.2 Controversial application

Further attempts to quantify RNA isolated from FFPE samples, however, have been more controversial. To this end, most researchers are suspicious about quantification results generated by RNA isolated from FFPE samples because less is known about how fixation delay , time of fixation, RNA half life, storage time affects the results of these quantification assays. And there is a lack of systematic studies to address the question of whether quantifying RNA from FFPE samples can generate meaningful expression information. Some of the in depth studies performed in this area are summarized below:

1.7.2.1 qRT-PCR platform

When FFPE-derived RNAs are used on qRT-PCR platform, every RNA fragmentation that occurs between two priming locations inevitably separates the two ends of the amplicon into two different RNA molecules, and the RNA is therefore lost as template for subsequent PCR amplification, leading to increased threshold cycle (Ct values). In addition, heavily modified and cross linked RNA molecules are less favorable material for reverse transcriptase during cDNA synthesis. Technically speaking, it is still possible to quantify RNA derived from FFPE samples by reducing the amplicon size and using random priming in the RT step [62]. It has been demonstrated that even mRNA isolated from samples with a fixation delay of up to 24 hours, prolonged fixation time of up to 21 days, and stored at room temperature for years can be quantified successfully on qRT-PCR platform [62].

Absolute quantification of RNA expression levels or copy numbers is usually not indicated, because of loss of amplifiable RNA template due to autolysis during fixation delay, FFPE processing and continuous degradation at storage. Currently, it is impossible to predicate expression level before fixation based on quantification results from degraded RNA, because how those factors influence final results is not well studied, and factors such as fixation delay, storage conditions are mostly untraceable. To make absolute quantification even more difficult, RNA template reduction seems to vary from gene to gene [63]. For example, based on changes of Ct values, it has been shown that only 3%-30% of RNA fragments are available for quantification in FFPE samples, corresponding to a Ct shift between 1.8 to 5.1 cycles compared to frozen sample.

Although not suitable for absolute quantification, systematic studies showed RNA template reduction due to degradation and modification may be less important sources of

imprecision in inter individual comparison of relative expression levels, because target genes and housekeeping genes are equally affected in all samples. It has been demonstrated that the abundance of a gene relative to one or several reference genes is not changed significantly as long as an amplicon of less than 140bp is targeted [64]. However, unbalanced influence on genes and amplicons within the same transcript may pose a challenge when comparisons of different transcripts are performed, such as for mRNA splice variants [63].

1.7.2.2 Microarray platform

Today, profiling FFPE sample-derived RNA on array platform presents both an incredible opportunity and a great challenge. Standard array platforms are designed in a way that assumes high quality input RNA. For example, on commonly used mRNA expression array platform, probes are located about 600bp away from 3' end of transcript. Targets are prepared using a hybrid primer with oligo dT and T7 promoter sequence to transcribe mRNA into double stranded cDNA for one or more rounds of amplification *in vitro*. These tactics work fine with high quality RNA, which has intact poly A tails and an average fragment size above 1KB. However, it is more problematic for highly fragmented and modified RNA isolated from FFPE samples. Highly degraded and modified poly A tails pose first barrier for hybrid primer annealing and cDNA synthesis. Even if RNA is successfully converted into double stranded cDNA and amplified, it may not be detected by probes which are upstream of sites of mRNA fragmentation.

It was first reported that mRNA profiling could be performed from formalin fixed and routinely paraffin embedded gastric carcinomas biopsy samples using a cDNA microarray. A global correlation coefficient of 0.718 was found between FFPE samples

19

and unfixed frozen control samples [65]. Using the paradise system, a linear amplification method designed to profile degraded RNA, a higher correlation (0.80-0.97) was reported by Renana et al using the Agilent oligonucleotide microarray platform [66]. However, the amount of information lost due to FFPE processing hasn't been further investigated. Recently, on an Affymetrix platform, it has been shown that profiling FFPE sample-derived RNA could reliably identify the p38 modulated pathways comparing to frozen counterpart array [67]. In another study, it has been shown that at least 24% of unselected FFPE tumor samples with an age of 2 to 8 years produce RNA of sufficient quality for standard microarray analysis; unsupervised clustering was able to distinguish tumor types and identify origin of unclassified tumor [68]. Although these studies showed the promising potential and possible applications of profiling mRNA extracted from FFPE samples, the representativeness of these conclusions are questionable. In most of these studies, immediately fixed FFPE samples were used for RNA extraction shortly after FFPE processing, thus RNA fragmentation was intentionally avoided, which may not reflect the actual processing of samples in a clinical setting. The global correlation between optimally processed FFPE sample and their frozen counterpart ranged from 0.72~0.97 [65] [66]. If one takes into account unbalanced profile distortion introduced by fixation delay, overfixation and degradation at storage, the correlation for most unselected routinely processed FFPE samples to its frozen sample is expected to be lower. Indeed, our previous data (not published) has shown a lower average correlation (0.66) when routinely processed FFPE samples in a clinical setting are studied. More recently, platforms designed to cope with mRNA fragmentation have emerged such as Illumina's DASL system, NuGene's whole transcriptome amplification on the

Affymetrix array platform, whose robustness and ability to generate meaningful mRNA profile is yet to be validated in the future.

Like mRNA, there is growing interests in profiling miRNAs on microarray platform. Currently, the survivability and expression level changes of miRNA during FFPE processing are largely unknown, however, it is assumed that the small sizes of miRNAs as well as their relative stability may render them less vulnerable comparing to mRNAs during FFPE processing, making it possible to generate meaningful profiles from FFPE samples. Indeed, initial studies have shown consistently good correlation between matched frozen and FFPE miRNA profiles using either RNA-primed, array-based Klenow enzyme (RAKE) microarray platform [69], or locked nucleic acid (LNA) based miRNA arrays [70].

1.8 Research objective

To discover functions of RNAs within the framework of biological networks, large scale gene expression analysis needs to be performed. Archival FFPE samples, with well annotated clinical information, could be invaluable tissue source for gene expression profiling. In spite of all effects of previous studies, it remains unclear to what extent mRNA/miRNA isolated from routinely processed FFPE samples can be used on current RNA quantification platforms. Comparing RNA quantification results generated from matched frozen and FFPE samples would provide insight into these unanswered questions.

Here, we hypothesized that FFPE-derived RNA retains considerable gene expression information despite fragmentation and modification of RNA molecules during FFPE processing. Two objectives in this project were:

1) Study miRNA profile on microarray platform using RNA isolated from FFPE samples, and compare to profiles generated from matched frozen samples.

2) Study mRNA profile on standard microarray platform using RNA isolated from FFPE samples, and compare to profiles generated from matched frozen samples.

CHAPTER 2 Materials and Methods

2.1 Global profiling of miRNAs isolated from FFPE samples

2.1.1 Sample collection

Matched frozen and FFPE samples of lymph node hyperplasia tissues were obtained from the Department of Pathology and Molecular Medicine, Kingston General Hospital (Ontario, Canada). Snap frozen samples were embedded in Optimal Cutting Temperature freezing medium (OCT) and stored at -80°C until use. FFPE samples were made following routine formalin fixation and paraffin embedding protocols and stored at room temperature until use. Tissue samples contained at least 75% lymphoid tissue without necrosis as confirmed by Dr LeBrun, hematopathologist, Queens University. Sample age ranged from one to two years. Seven anonymous paired lymphoid hyperplasia tissues were studied.

2.1.2 RNA extraction

The miRNeasy kit (Qiagen, Mississauga,Canada) was used to extract total RNA (including miRNA) from frozen samples. About 30mg of frozen tissue was disrupted using a tissue homogenizer in the presence of QIAzol lysis reagent. Following a chloroform extraction, the aqueous phase was added to a column, and RNA eluted in 60 µl of water. The RecoverAll total RNA Isolation kit (Ambion, Streetsville, Canada) was used to extract total RNA (including miRNA) from FFPE samples. Three 20µm slices were deparaffined with xylene, washed twice with ethanol, and digested with protease at 50ºC for 3 hours. The lysate was passed through a filter cartridge and RNA eluted in 60µl of water. The quality of each sample was checked using the Agilent 2100 Bioanalyzer (Agilent, Santa Clara,

CA), with RNA quality represented by the RIN(RNA integrity number, ranges from 1-10, with 10 representing intact RNA). The RIN is derived from measurements of areas under the peaks of the large ribosomal RNAs compared to the area under the remaining trace for each RNA sample).

2.1.3 miRNAs expression profiling

miRNAs were labeled using the Agilent miRNA labeling reagent and hybridized to Agilent human miRNA arrays. In brief, 100ng total RNA was dephosphorylated and ligated with pCp-Cy3. Labeled RNA was purified and hybridized to Agilent miRNA arrays with eight identical arrays per slide, with each array containing probes interrogating 470 human miRNAs. Triplicate arrays were performed for two pairs of hyperplasia samples and duplicate arrays for three pairs of hyperplasia samples. Images were scanned with the Agilent microarray scanner (Agilent, Santa Clara, CA), which were then gridded and analyzed using Agilent feature extraction software Version 9.5.3.

2.1.4 Statistical analysis

Raw feature intensity was first log 2 transformed, and then interarray normalized by Z score transformation using SPSS 16.0 software (SPSS, Chicago, IL) such that mean=0 and std=1 for each array. All following analyses were done on normalized log transformed intensity values.

14 frozen samples and 14 matched FFPE samples were averaged respectively. For each miRNA, fold signal change between frozen and FFPE samples was calculated using the formula: signal change in fold $= 2^{(\text{averaged FFPE samples- averaged frozen samples})}$.

Each matched frozen and FFPE samples was line plotted together for visual comparison.

Parametric and non parametric correlation analysis methods (Pearson correlation coefficient, Kendall tau and Spearman rank correlation coefficient) were calculated to investigate the similarity of expression profiles between matched frozen and FFPE samples. Pearson correlation, Kendall tau and Spearman rank correlation coefficients were calculated between technical replicates using either same tissue sample, or same RNA pool on same/different slides to assess the variations introduced by miRNA extraction, labeling & hybridization and slide heterogeneity.

2.2 Global profiling of mRNAs isolated from FFPE samples

2.2.1 RNA extraction

Matched frozen and FFPE samples of lymph node hyperplasia tissues were obtained from the Department of Pathology and Molecular Medicine, Kingston General Hospital (Ontario, Canada). Snap frozen samples were embedded in Optimal Cutting Temperature freezing medium (OCT) and stored at -80°C until use. FFPE samples were made following routine formalin fixation and paraffin embedding protocols and stored at room temperature until use. Tissue samples contained at least 75% lymphoid tissue without necrosis as confirmed by Dr Lebrun. Sample age ranged from 1.5 to 2 years. Four anonymous paired lymphoid hyperplasia tissues were investigated.

2.2.2 RNA extraction

The RNeasy kit (Qiagen, Mississauga,Canada) was used to extract total RNA from OCT embedded frozen samples. The Optimum^{TM} FFPE RNA isolation kit (Ambion diagnostics, Austin, TX) was used to extract total RNA from FFPE samples. In brief, 10µm slice were deparaffined with xylene, washed twice with ethanol, and digested with

protease K at 37ºC for 3 hours. The lysate was passed through a filter cartridge and RNA eluted in TE buffer (pH=8.0). The quality of each sample was checked using an Agilent 2100 Bioanalyzer (Agilent, Santa Clara, CA)..

2.2.3 pH and temperature optimization

2μg of intact human tonsil total RNA (BD Bioscience, ON, Canada) at a concentration of 1μg/ μl was added into 6 μl buffer solution with various pH (pH 3-8), then heated at various temperatures (65°C-75°C) for 30 minutes in PTC-200 thermal cycler (Bio-Rad, Hercules, CA). 2 μg of intact human tonsil total RNA was added into 6 μl nuclease free water as an untreated control. Samples were precipitated and resuspended in 4.5 μl nuclease free water, and the quality of RNA was assessed using a Nanochip assay on the Agilent 2100 Bioanalyzer (Agilent, Santa Clara, CA).

1 μg total RNA isolated from a lymphoid hyperplasia FFPE sample (sample ID 05-10508) was precipitated with ethanol and resuspended in buffer with various pH (pH 3-8). RNA was treated at 75°C for 30 minutes in PTC-200 thermal cycler (Bio-Rad, Hercules,CA) followed by precipitation and resuspension in 8μl nuclease free water. 1 μg total RNA from same RNA pool was precipitated followed by resuspension in 8 μl nuclease free water as an untreated control. RNA concentration was measured using a Nanodrop spectrophotometer ND-1000 (Nanodrop, Wilmington, DE). 300ng total RNA from either treated samples or untreated control were reverse transcribed into cDNA using Superscript III (Invitrogen, Burlington, Canada).

1 μg total RNA isolated from lymphoid hyperplasia FFPE sample (sample ID 05-10508) was treated for 60 minutes at various temperatures (60°C-100°C) in PTC-200 thermal cycler (Bio-Rad, Hercules,CA,USA). 300ng total RNA from either treated samples or

untreated control were reverse transcribed into cDNA using Superscript III (Invitrogen, Burlington, Canada).

Primer sets targeting β-actin were designed to amplify 250bp, 328bp, 511bp and 650bp amplicons(Table 2-1). PCR was performed as shown in Table 2-2.

Target gene	Amplicon length	Forward primer	Reverse primer
β-actin	250 nt	GGCATCCACGAAACTACCTT	ACATCTGCTGGAAGGTGGAC
β-actin	328 nt	CCCAGCACAATGAAGATCAA	CACCTTCACCGTTCCAGTTT
β-actin	511 nt	CACCTTCACCGTTCCAGTTT	CTCTCCCAGCCTTCCTTCCT
β-actin	650 nt	GCTATCCCTGTACGCCTCTG	ACATCTGCTGGAAGGTGGAC

Table 2-1. Oligonucleotide primer sequences for RT-PCR. Sequences are given 5' to 3' for all primers.

Reagents	Amount in the mix
Nuclease Free Water	17.03 µl
10 × PCR Buffer	2.5 µl
50mM MgCl$_2$	0.84 µl
10mM dNTPs	0.5 µl
20µM Forward primer	1 µl
20µM Reverse primer	1 µl
RT reaction mix	2 µl
Taq Recombinant (Invitrogen, Burlington, Canada)	0.13 µl
Total Volume	25 µl

Table 2-2. PCR conditions used for RT-PCR reactions. The PCR consisted of an initial incubation at 94°C for 3 minutes, followed by 40 cycles of 94°C for 30 s, 53°C for 30 s, 72°C for 30 s, and a final extension step at 72°C for 7 minutes.

2.2.4 Heat treatment of FFPE derived RNA

100ng total RNA isolated from each FFPE lymphoid hyperplasia sample was put into each of three tubes. Two were treated for 1 hour at 80°C or 86°C respectively, and the

third left unheated. Therefore, each pair of matched samples produced one fresh sample derived RNA, one untreated FFPE sample derived RNA and two treated FFPE sample derived RNAs.

2.2.5 mRNA amplification

2ng total RNA from frozen sample and 10ng total RNA from matched FFPE samples, either untreated or treated, were linearly amplified to generate cRNA using RiboAmp HS kit (Acturus, Sunnyvale, CA). Amplified cRNA was quantified using a Nanodrop spectrophotometer ND-1000 (Nanodrop, Wilmington, DE).

2.2.6 mRNA labeling

6-10 μg cRNA was labeled with Cy3 using Acturus Turbo Cy3 labeling kit (Acturus, Sunnyvale, CA). Yield and Cy3 labeling efficiency of cRNA were assessed using a Nanodrop spectrophotometer ND-1000 (Nanodrop, Wilmington, DE). Only samples with a cRNA yield >1.65μg and frequency of dye incorporation (FOI)>20 proceeded to array hybridization.

2.2.7 Hybridization

1.65μg labeled cRNA was hybridized in a rotating oven to the Agilent 4×44K Human Whole Genome microarray following the Agilent one color gene expression microarray protocol (version 5.5). This array platform has four identical arrays per slide, each contains approximate 44K probes interrogating whole human genome. Frozen sample RNA, untreated FFPE sample RNA, FFPE sample RNA treated at 80° C, and FFPE sample RNA treated at 86°C were profiled in that order on a single slide. Images were

scanned with the Agilent microarray scanner (Agilent, Santa Clara, CA), which were then gridded and analyzed using Agilent feature extraction software Version 9.5.3.

2.2.8 Statistical analysis

Saturated features (raw data $\geq$ 65,000 pixels) were removed from analysis. A lower background noise threshold was determined based on a histogram of each individual array. In brief, a cut off value was determined visually which removed the cluster at the lower end of histogram (representing background noise). Any feature with intensity equal to or lower than the threshold was removed.

Before array data analysis, interarray normalization is routinely performed to reduce biases introduced by experimental manipulations such as input RNA variation, labeling and hybridization differences and array manufacturing heterogeneity. Failure to properly normalize data used in microarray comparisons could produce highly skewed results, reducing the credibility of conclusions [71]. One commonly used approach is global normalization, which calculates the mean or median of the raw intensities of each individual array. Each data set is then mathematically adjusted such that the mean or median of dataset is equal to a constant. The principle of this approach assumes that majority of gene expression information on array platform remains relatively constant under the experimental conditions [72]. Although global normalization holds true where experimental conditions only cause expression changes of limited genes, it may not be applicable in our situation, since FFPE processing and heat treatment are expected to cause global, imbalanced signal changes on the array platform. Furthermore, highly fragmented and modified RNA may greatly increase the likelihood of non specific hybridization on standard array platform, resulting in a high level of noise. To our

knowledge, no existing interarray normalization solution is able to tackle such complex situations as in our study. We did employ a log (base2) transformation on the data to calculate correlations between the datasets (see below). However, investigations in enhanced features was done only using raw intensity values because of the nature of the question we were asking, which was whether the FFPE-derived RNA could be improved at the raw technical level by our treatments.

The intensity of each feature in the frozen samples was compared to untreated FFPE sample, a feature was defined as decreased if raw intensity of frozen sample was at least 50 pixels stronger than untreated FFPE sample.

The intensity of each feature in the treated FFPE samples was compared to untreated FFPE sample. A feature was defined as enhanced if raw intensity of treated FFPE sample was at least 50 pixels stronger than untreated FFPE sample; not enhanced if intensity difference between treated and untreated FFPE sample was no larger than 50 pixels; decreased if intensity of treated FFPE sample was at least 50 pixels lower than untreated FFPE sample.

To determine whether heat treatment was enhancing features by chance, the number of features enhanced by heat treatment was estimated using the formula (total number of features × possibility of being enhanced by 80° C treatment × possibility of being enhanced by 86° C treatment), assuming enhancement occurred totally independent under these two conditions. Estimated numbers were compared to observed number of features enhanced by both treatments, and p values calculated to assess the possibility that estimated numbers and actual observed numbers were from same population using the formula p(observed, expected) = 1-erf[(observed-expected)/sqrt(2*expected)]. The cutoff

value defining a feature as being enhanced was then raised to 100 pixels, 500 pixels and 1000 pixels and the same analysis repeated.

The 10, 100, 500, 1000 most enhanced and decreased features by 80° C treatment (50 pixels as cutoff value) were then compared using Students t test to examine the influence of transcript abundance and probe GC content on effects of treatment.

Spearman rank correlation coefficients were used to investigate correlation changes due to the treatment between matched frozen and FFPE samples. Here, the correlation analysis was performed using log transformed raw intensity.

CHAPTER 3 Profiling miRNAs Isolated From FFPE Samples

3.1 RNA quantity and quality

Both frozen and matched FFPE samples yielded enough total RNA (5μg-30μg) for miRNA profiling. The quality check showed that the frozen samples retained miRNA peak(18-24nt), while the same peak in FFPE sample was obscured by small size degraded mRNAs ,tRNAs and rRNAs (Fig3-1), consistent with previous observation [45] [57] .

3.2 miRNA signal difference between frozen and FFPE samples

416 out of 470 FFPE sample-derived miRNAs (88.5%) showed no larger than 0.1 fold signal change from frozen sample. Almost all FFPE sample-derived miRNAs (99.6%, 468 out of 470) showed no large than 1 fold signal change. Only two outlying data were found (miR-142-5p signal decreased more than 1 fold, miR-638 signal increased more than 1 fold).

3.3 Variation Due to Labeling and Hybridization

To identify variations that might be introduced at the labeling and hybridization steps, we analyzed the correlations of four pairs of duplicate arrays performed on the same slide. Results showed that duplicate arrays using a common RNA were highly correlated (Fig 3-2) (Pearson correlation coefficient=0.995-0.999,Kendall tau=0.804-0.853, Spearman rank correlation coefficient=0.924-0.954, p values for all correlation analyses <0.01).

3.4 Variation Due to RNA Extraction

To examine variations due to the RNA extraction, we compared arrays on the same slide hybridized with miRNA isolated separately from the same tissue. Results showed

duplicate arrays using separate preparations of RNA from the same tissue source were highly correlated (Pearson correlation coefficient=0.978-0.999, Kendall tau=0.722-0.847, Spearman rank correlation coefficient= 0.921-0.949, p values for all correlation analyses <0.01) (Fig 3-3).

3.5 Slide Variation

To assess slide to slide variation, we compared arrays on different slides using miRNAs extracted separately from the same sample. The results showed a slightly lower correlation (Pearson correlation coefficient=0.913-0.954, Kendall tau=0.727-0.757, Spearman rank correlation coefficient=0.891-0.912, p values for all correlation analyses <0.01) (Fig 3-4).

3.6 Correlation of miRNA Expression Profiles Between Matched Frozen and FFPE Samples

Because triplicate arrays were performed for two pairs of hyperplasia samples and duplicate arrays for three pairs of hyperplasia samples, we had 32 comparisons between matched frozen and FFPE samples. Good correlations were found in all 32 comparisons (Pearson correlation coefficient=0.885-0.980, Kendall tau=0.669-0.815, Spearman rank correlation coefficient=0.847-0.948, p values for all correlation analyses <0.01)(Table3-1). Results from the three correlation analysis methods matched each other well. Scatter plots for matched sample pairs with the best and worst correlations are shown in Fig 3-5. Correlation analysis for each pair of sample was summarized in Table 3-2 (frozen vs. frozen/ FFPE vs. FFPE/ frozen vs. FFPE).

3.7 Similarity of Individual miRNA Between Matched Frozen and FFPE Samples

After performing a Z score transformation to reduce the systemic biases between arrays, a line plot was used to visually inspect the difference between individual miRNA expression levels in matched samples (Fig 3-6). Results suggested that miRNAs isolated from FFPE samples retain most of the characteristic expression pattern of the frozen counterpart. In cases where the FFPE-derived miRNA deviated from the frozen sample profile, no fixed pattern was found.
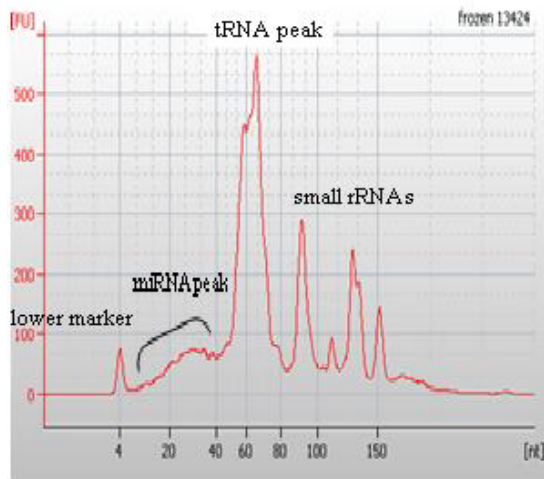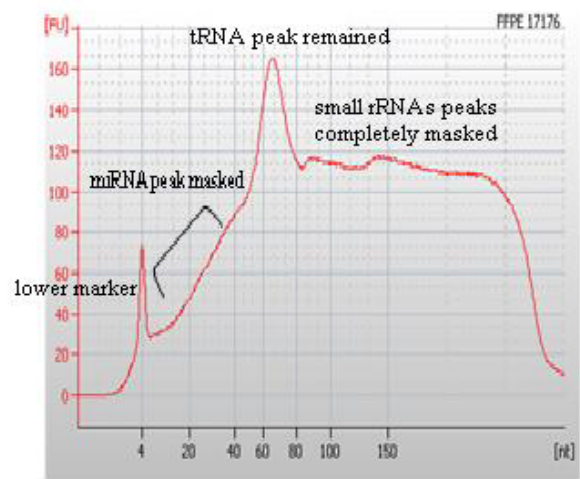
Figure 3-1. Effects of formalin fixation and paraffin embedding on miRNA. (A) Frozen sample derived total RNA electrophorogram on Agilent Bioanalyzer small RNA chip. The miRNA peak is clearly present and is indicated, as are peaks from other populations of small RNAs .(B) FFPE derived total RNA electrophorogram on Agilent Bioanalyzer small RNA chip. The miRNA peak and small rRNAs peaks are masked by degraded longer RNA molecules.

A
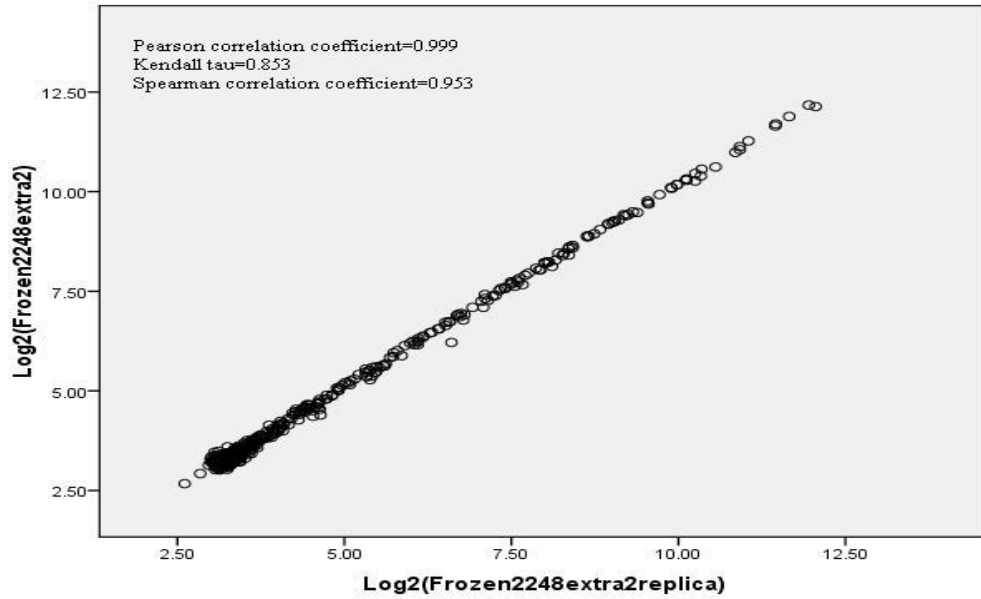
B
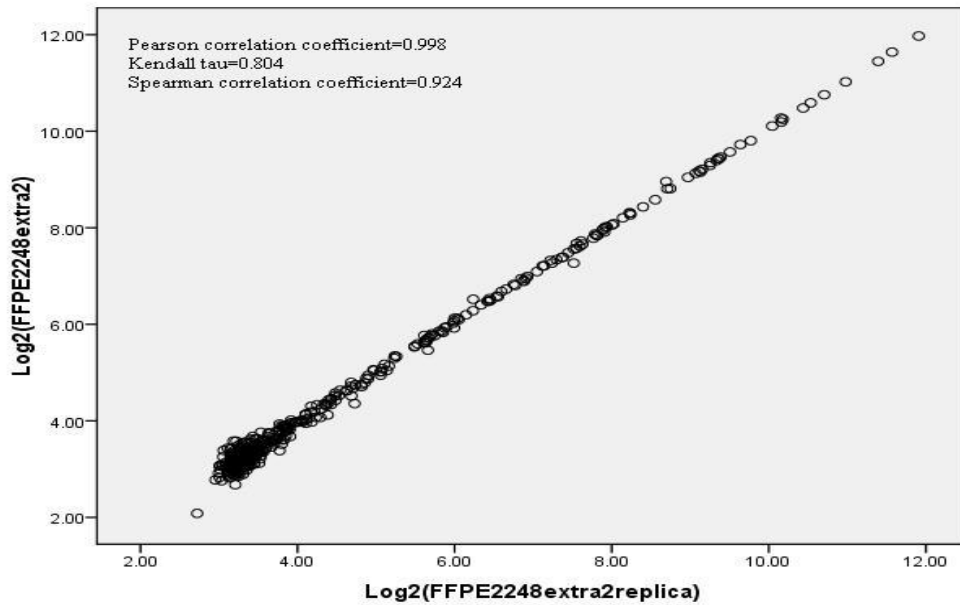
Figure 3-2: Scatter plots of technical replicate arrays starting with the same RNA pool, separately labeled and hybridized to arrays on the same slide. The high correlations suggest that labeling and hybridization are highly reproducible. (A) Scatter plot of replica frozen sample arrays(Frozen2248extra2 vs. Frozen2248extra2 replica). (B) Scatter plot of replica FFPE sample arrays(FFPE2248extra2 vs. FFPE2248extra2 replica). Scatter plots are derived from log (base 2) transformed data.

A
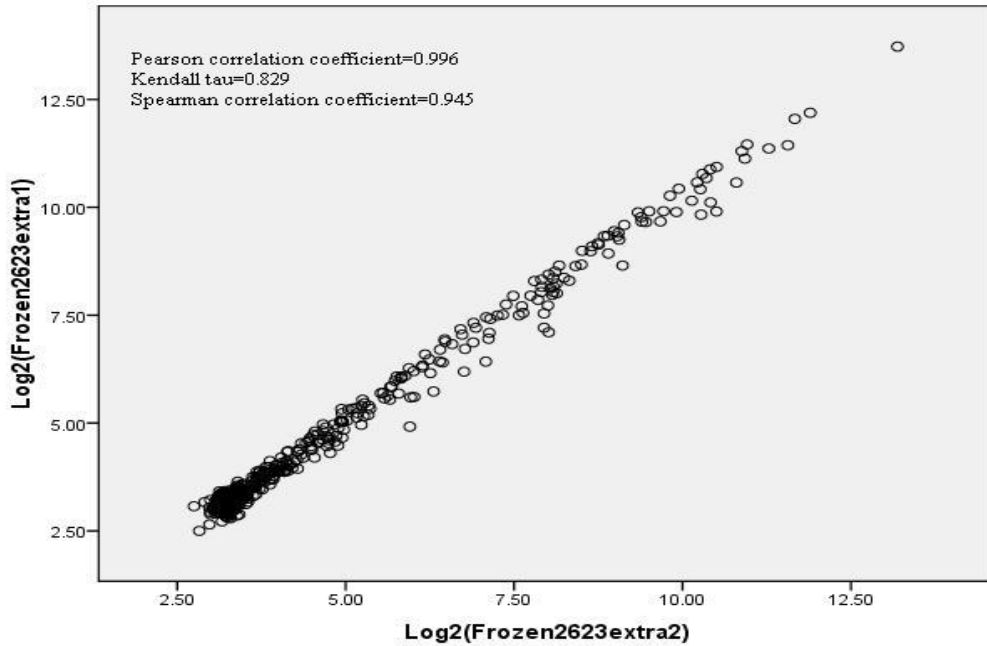
B
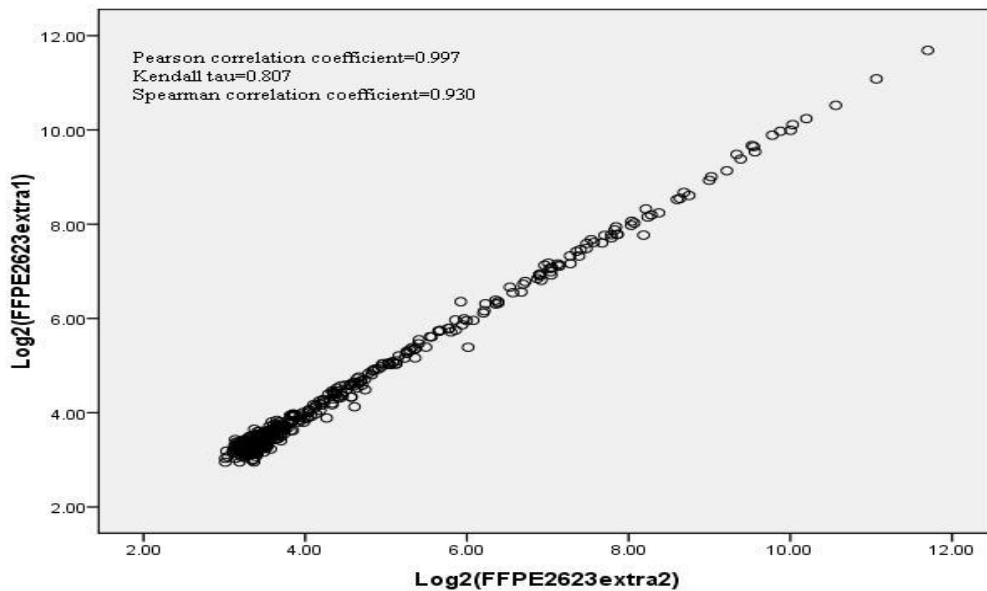
Figure 3-3: Scatter plots of technical replicate arrays starting with the same tissue sources. RNA samples were separately extracted, labeled and hybridized to arrays on the same slide. The high correlations suggest that RNA extraction, labeling and hybridization processes are highly reproducible. (A) Scatter plot of replica frozen sample arrays(Frozen2623extra1 vs. Frozen2623extra2). (B) Scatter plot of replica FFPE sample arrays(FFPE2623extra1 vs. FFPE2623extra2). Scatter plots are derived from lg (base 2) transformed intensity data.

A
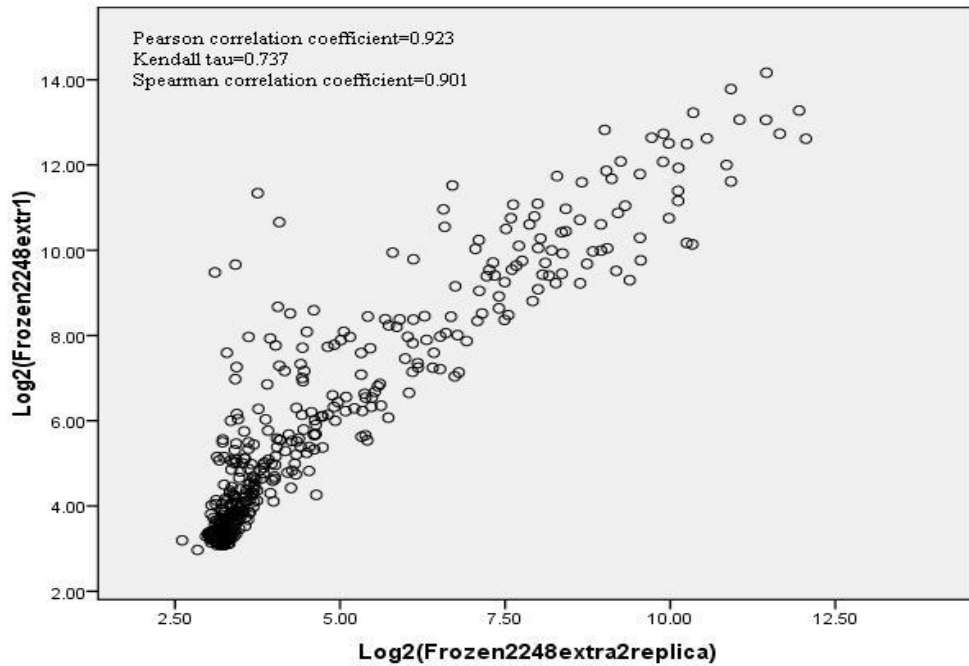
B
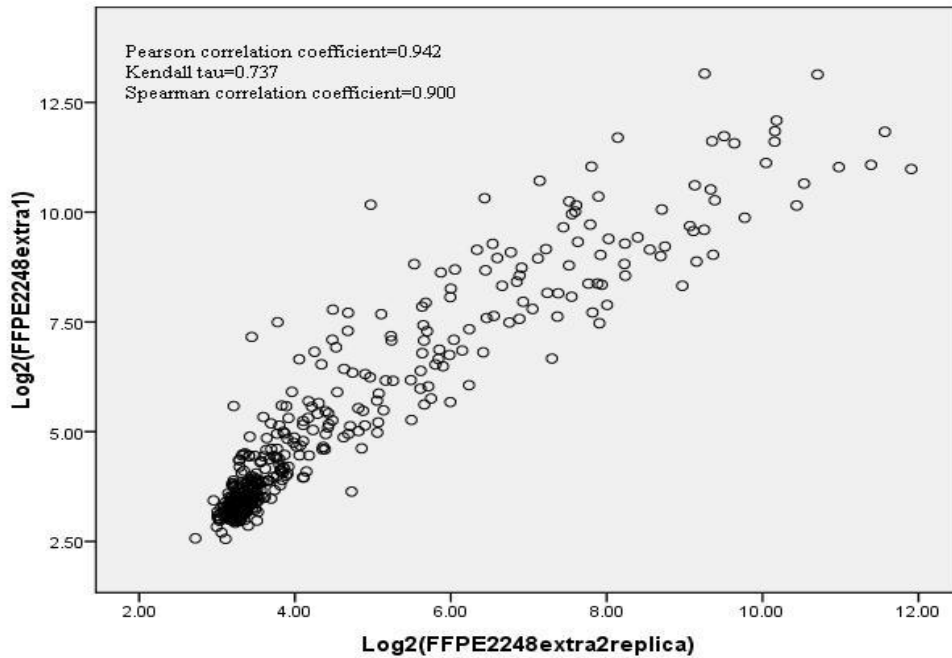
Figure 3-4: Scatter plots of technical replicate arrays starting with same tissue scource.RNA was separately extracted, labeled and hybridized to arrays on different slides. The high correlations suggest that RNA extraction, labeling and hybridization are highly reproducible, but that slide to slide variation is greater. (A) Scatter plot of replica frozen sample arrays(Frozen2248extra1 vs. Frozen2248extra2 replica). (B) Scatter plot of replica FFPE sample arrays(FFPE2248extra1 vs. FFPE2248extra2 replica). Scatter plots are derived from log (base2) transformed intensity data.

A
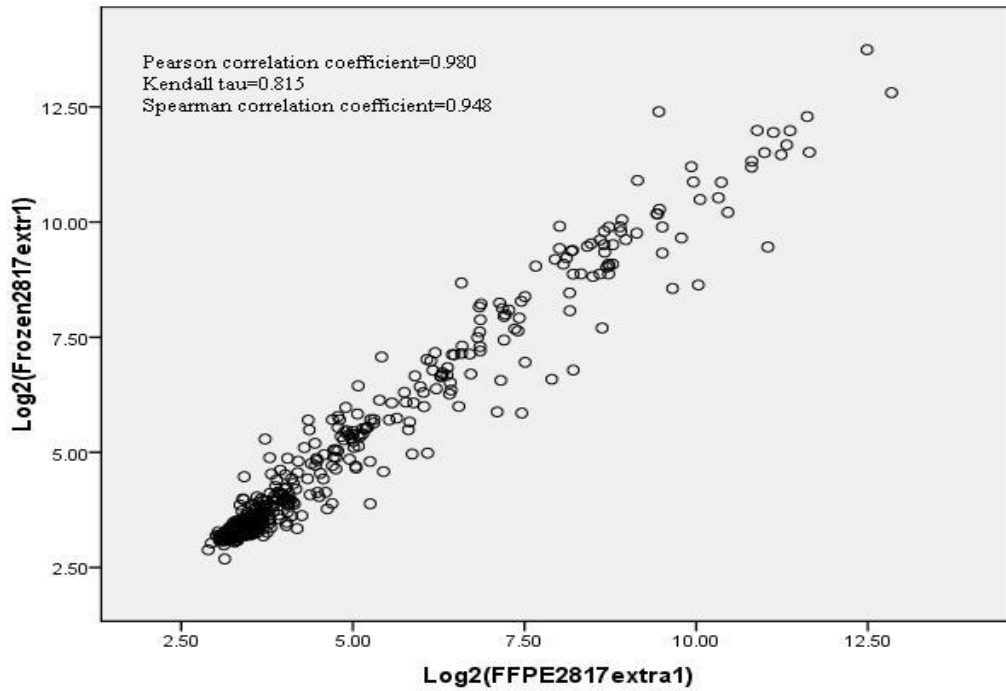
B
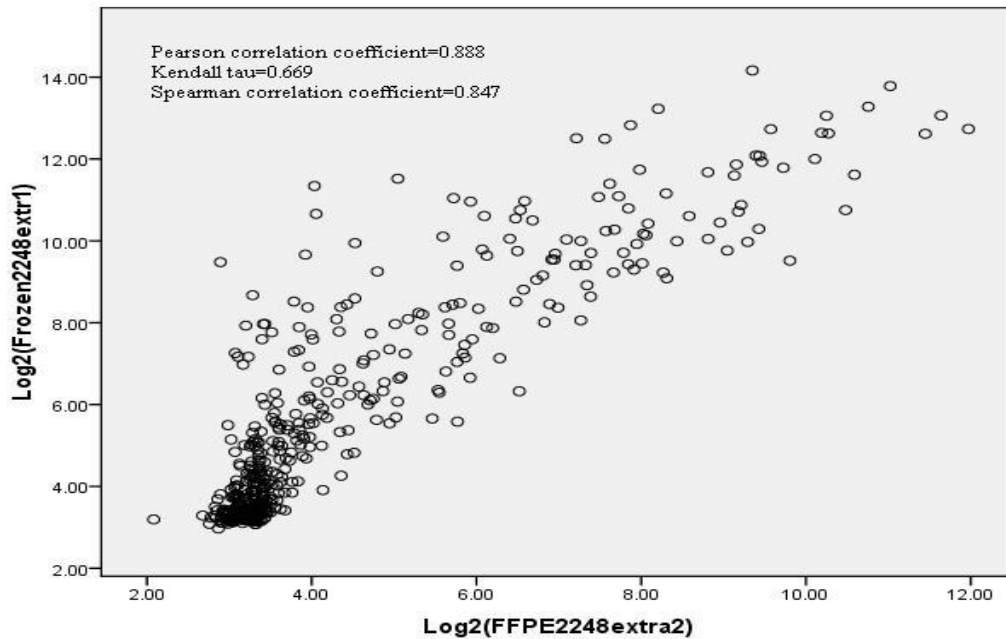
Figure 3-5. Scatter plots of frozen sample array vs. matched FFPE sample array. (A) Scatter plot of the best correlated sample pair (Frozen2817extra1 vs.FFPE2817extra1). (B) Scatter plot of the poorest correlated sample pair(Frozen2248extra1 vs.FFPE2248extra2) .In both cases, significant high correlations were found between matched samples. Scatter plots are derived from log (base2) transformed intensity data.
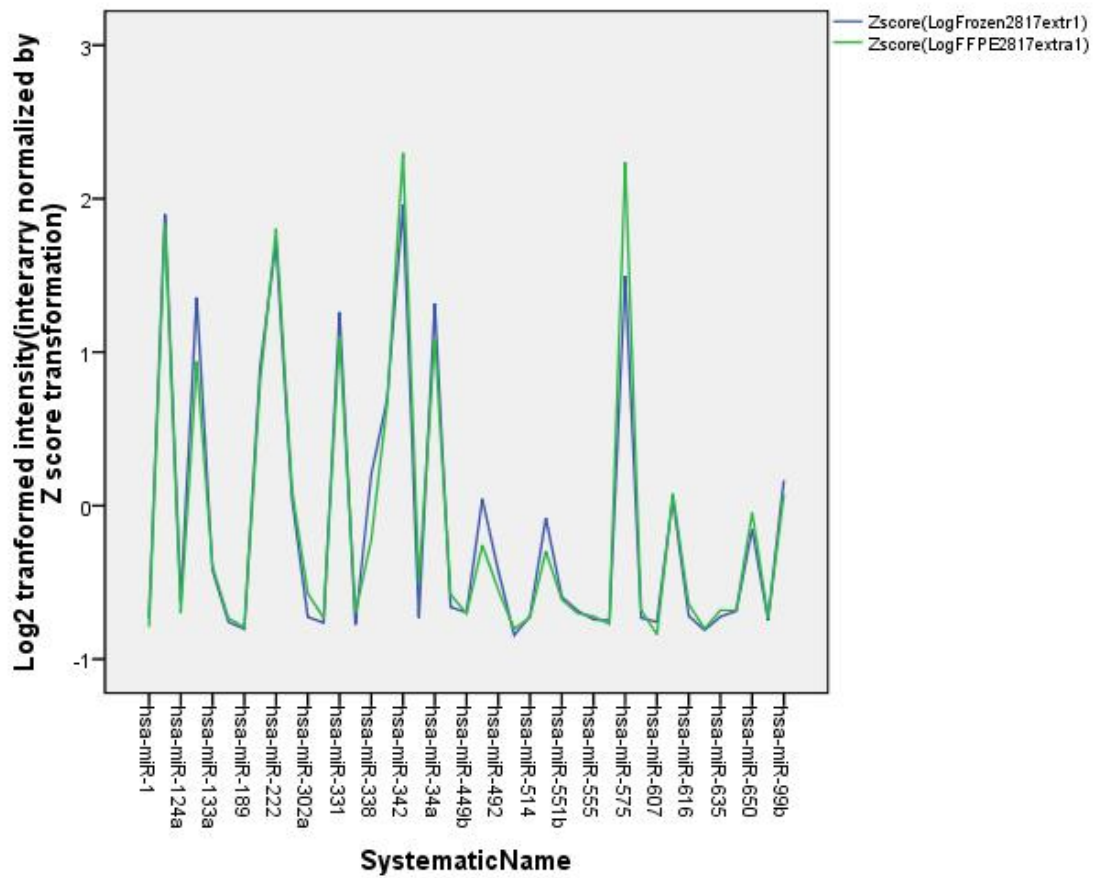
Fig 3-6: Line plot of 30 randomly chosen miRNAs comparing the Z score transformed log(base2) intenties of matched frozen sample and FFPE sample. Overall, the FFPE sample miRNA profiles match that of the frozen sample.

	Mean	Minimum	Maximum	Std. Deviation
Kendall tau	0.744	0.669	0.815	0.033
Spearman coefficient	0.905	0.847	0.948	0.024
Pearson correlation coefficient	0.939	0.885	0.98	0.026

	Kendall tau	Spearman coefficient	Pearson coefficient
Sample 06-2817	0.815**	0.948**	0.98**
Sample 05-11903	0.716	0.89	0.924
Sample 06-17176	0.798	0.942	0.95
	0.778	0.931	0.947
	0.759	0.917	0.947
	0.726	0.897	0.912
	0.747	0.908	0.916
	0.743	0.905	0.921
	0.704	0.875	0.902
	0.702	0.871	0.902
	0.689	0.862	0.908
Sample 07-2248	0.782	0.929	0.947
	0.669*	0.847*	0.888
	0.683	0.856	0.885*
	0.76	0.917	0.956
	0.755	0.909	0.964
	0.76	0.911	0.964
	0.747	0.909	0.954
	0.723	0.883	0.964
	0.752	0.905	0.964
Sample 05-11826	0.724	0.897	0.917
	0.721	0.895	0.906
	0.737	0.906	0.932
	0.746	0.913	0.921
Sample 05-19322	0.783	0.93	0.966
	0.761	0.917	0.964
	0.761	0.915	0.966
	0.758	0.913	0.964
Sample 05-2623	0.761	0.921	0.947
	0.742	0.908	0.945
	0.75	0.913	0.958
	0.769	0.924	0.957

Table 3-1: Kendall tau , Spearman rank correlation and Pearson correlation coefficient of
32 comparisons between matched frozen sample array and FFPE sample array.
** best correlation .
*   worst correlation .

Pearson coefficient

	sample06-2817			sample 05-11903			sample 06-17176			sample 07-2248			sample 05-11826			sample 05-19322			sample 05-2623		
	Fr vs. Fr	FF vs. FF	Fr vs. FF	Fr vs. Fr	FF vs. FF	Fr vs. FF	Fr vs. Fr	FF vs. FF	Fr vs. FF	Fr vs. Fr	FF vs. FF	Fr vs. FF	Fr vs. Fr	FF vs. FF	Fr vs. FF	Fr vs. Fr	FF vs. FF	Fr vs. FF	Fr vs. Fr	FF vs. FF	Fr vs. FF
			0.980			0.924	0.929	0.954	0.950	0.926	0.944	0.947	0.994	0.998	0.917	0.978	0.997	0.966	0.996	0.997	0.947
							0.913	0.951	0.947	0.923	0.942	0.888			0.906			0.964			0.945
							0.995	0.997	0.947	0.999	0.998	0.885			0.932			0.966			0.958
									0.912			0.956			0.921			0.964			0.957
									0.916			0.964									
									0.921			0.964									
									0.902			0.954									
									0.902			0.964									
									0.908			0.964									
Mean	N/A	N/A	0.980	N/A	N/A	0.924	0.946	0.967	0.923	0.949	0.961	0.943	0.947	0.949	0.919	0.921	0.936	0.965	0.945	0.930	0.952
std dev	N/A	N/A	N/A	N/A	N/A	N/A	0.043	0.026	0.020	0.043	0.032	0.033	N/A	N/A	0.011	N/A	N/A	0.001	N/A	N/A	0.007

Spearman coefficient

	sample06-2817			sample 05-11903			sample 06-17176			sample 07-2248			sample 05-11826			sample 05-19322			sample 05-2623		
	Fr vs. Fr	FF vs. FF	Fr vs. FF	Fr vs. Fr	FF vs. FF	Fr vs. FF	Fr vs. Fr	FF vs. FF	Fr vs. FF	Fr vs. Fr	FF vs. FF	Fr vs. FF	Fr vs. Fr	FF vs. FF	Fr vs. FF	Fr vs. Fr	FF vs. FF	Fr vs. FF	Fr vs. Fr	FF vs. FF	Fr vs. FF
			0.948			0.890	0.909	0.935	0.942	0.912	0.891	0.929	0.947	0.949	0.897	0.921	0.936	0.930	0.945	0.930	0.921
							0.874	0.921	0.931	0.901	0.900	0.847			0.895			0.917			0.908
							0.933	0.954	0.917	0.953	0.924	0.856			0.906			0.915			0.913
									0.897			0.917			0.913			0.913			0.924
									0.908			0.909									
									0.905			0.911									
									0.875			0.909									
									0.871			0.883									
									0.862			0.905									
Mean	N/A	N/A	0.948	N/A	N/A	0.890	0.905	0.937	0.901	0.922	0.905	0.896	0.947	0.949	0.903	0.921	0.936	0.919	0.945	0.930	0.917
std dev	N/A	N/A	N/A	N/A	N/A	N/A	0.030	0.017	0.027	0.027	0.017	0.028	N/A	N/A	0.008	N/A	N/A	0.008	N/A	N/A	0.007

Kendall tau

	sample06-2817			sample 05-11903			sample 06-17176			sample 07-2248			sample 05-11826			sample 05-19322			sample 05-2623		
	Fr vs. Fr	FF vs. FF	Fr vs. FF	Fr vs. Fr	FF vs. FF	Fr vs. FF	Fr vs. Fr	FF vs. FF	Fr vs. FF	Fr vs. Fr	FF vs. FF	Fr vs. FF	Fr vs. Fr	FF vs. FF	Fr vs. FF	Fr vs. Fr	FF vs. FF	Fr vs. FF	Fr vs. Fr	FF vs. FF	Fr vs. FF
			0.815			0.716	0.739	0.788	0.798	0.757	0.727	0.782	0.834	0.842	0.724	0.772	0.817	0.783	0.829	0.807	0.761
							0.693	0.771	0.778	0.737	0.737	0.669			0.721			0.761			0.742
							0.808	0.849	0.759	0.853	0.804	0.683			0.737			0.761			0.750
									0.726			0.760			0.746			0.758			0.769
									0.747			0.755									
									0.743			0.760									
									0.704			0.747									
									0.702			0.723									
									0.689			0.752									
Mean	N/A	N/A	0.815	N/A	N/A	0.716	0.747	0.803	0.738	0.782	0.756	0.737	0.834	0.842	0.732	0.772	0.817	0.766	0.829	0.807	0.756
std dev	N/A	N/A	N/A	N/A	N/A	N/A	0.058	0.041	0.037	0.062	0.042	0.038	N/A	N/A	0.012	N/A	N/A	0.012	N/A	N/A	0.012

Table 3-2 Summary of all correlation analyses (Pearson coefficient, Spearman coefficient and Kendall tau) of 7 pairs of matched frozen and FFPE samples (Fr=frozen sample, FF=FFPE sample). Correlations were calculated 1) between duplicate Frozen samples when applicable. 2) between duplicate FFPE samples when applicable and 3) between matched Frozen and FFPE samples. Standard deviations were calculated when possible. Note that different samples were examined in triplicate, duplicate or as single runs, depending on experimental design.

CHAPTER 4 Profiling mRNAs Isolated From FFPE Samples

4.1 RNA quantity and quality from frozen and FFPE samples

Both frozen and FFPE samples yielded enough total RNA (5μg-30μg) for cRNA amplification. RNA yield was unpredictable and generally lower in FFPE samples compared to matched frozen samples. No clear correlations were found between FFPE sample RNA yield and tissue size, amount or age, which agrees with previous findings [50]. RNA extracted from frozen samples showed clear 18S and 28S peaks on electrophorogram. FFPE sample-derived RNA showed a low hump towards low molecular weight on electrophorogram (Fig4-1), indicating extensive RNA fragmentation.

4.2 pH and temperature optimization

Using commercially available RNA, the effects of pH and temperature were investigated. We used commercially available RNA for initial optimization because of the difficulty of evaluating the additional degradation effects of the heat treatment on FFPE sample-derived RNA. RNA treated at pH 6 to 8 remained intact after treatment, while RNA treated at pH 3-5 degraded.(Fig 4-2).

When applied to FFPE sample-derived total RNA, the untreated control RNA and RNA treated at all pH conditions successfully supported the generation of up to 328 bp product after RT-PCR. For larger amplicons (>500bp), the effect of the pH for the heat treatment was evident, as only treatments using pH 6-8 supported the amplification of these larger products (Figure 4-3). Based on above data, it was concluded that pH 6-8 was the optimal pH range to treat the RNA, and pH 8.0 was chosen for convenience.

RNA treated at 60 °C to 84 °C showed relatively more product at 511bp after RT-PCR compared to untreated RNA. RNA treated at higher temperatures (>90°C) had relatively less product compared to untreated RNA (Fig 4-4). For the 650bp amplicon, results were inconsistent, suggesting that this size of amplicon was near the limit of the RNA fragment size. Therefore, we concluded that the optimal temperature was around 80°C. and 80°C and 86°C were selected for further work.

4.3 Microarray results

To assess the number of features enhanced by heat treatment, data was filtered to remove saturated features and low intensity features.Table4-1 shows the lower thresholds for each array, and number of features remaining after low intensity and saturated features were removed. Approximately 10,000 features on each array were left for analysis, accounting for about one third of the non control features.

4.3.1 Comparison between frozen and untreated FFPE samples

Frozen samples produced much stronger signals than untreated FFPE samples upon visual inspection in all pairs of samples. The average signal intensity of the frozen sample derived array was at least 30% higher than the corresponding untreated FFPE sample derived array. Signal decrease occurred in a non uniform manner across chip per feature. Feature percentage with at least 50 pixels higher intensity in frozen samples than untreated FFPE samples varied in four samples (98.6% in sample 05-19322, 78% in sample 05-10508, 43.2% in sample 05-13381 and 21.0% in sample 05-13947).

4.3.2 Comparison between untreated and treated FFPE samples

Visually, more features were evident using treated FFPE derived RNA compared to untreated FFPE derived RNA. The intensity of each feature from the treated FFPE sample was compared to that of the untreated FFPE sample. Results are shown in Table 4-2.

The actual number of enhanced features is greater than would be expected if the enhancement of features by heat treating was a random event. Raising the cutoff value defining a feature as being enhanced to 100 pixels, 500 pixels or 1000 pixels didn't change this conclusion although the percentage of enhanced features was lower with increasing cutoff value.

4.3.3 Difference between features enhanced and decreased

When the 10 most enhanced and most decreased features were compared, we found that the enhanced features had significantly higher raw intensity values in the frozen sample profile compared to the decreased features, with the mean intensity difference around 10000 pixels (Table 4-3). The same results were achieved when 100, 500, 1000 most enhanced and decreased features were examined, with an average feature intensity difference around 5000 pixels, 3000 pixels and 1000 pixels respectively.

A mixture of results was obtained when GC content of the probes corresponding to the enhanced features and decreased features were compared (Table 4-4).

4.3.4 Correlation changes after heat treatment

To investigate global effects of heat treatment on mRNA quality, the correlation between frozen and matched FFPE samples, untreated and treated, were analyzed and compared (table 4-5).The Spearman rank correlation coefficients between matched frozen and

untreated FFPE samples ranged from 0.522-0.712,consistent with previous data [65][70] .

After treatment, two samples (sample 05-10508, sample 05-13381) showed correlation increases greater than 0.1, while two other samples (sample 05-19322, sample 05-13947) showed a correlation change close to zero. Our data also showed that it's sample dependant which temperature treatment produced the most correlation improvement. For sample 05-10508, heat treatment at 80°C for one hour gave the best correlation improvement, for sample 05-13381, 86°C for 1 hour gave the best performance.

A

B
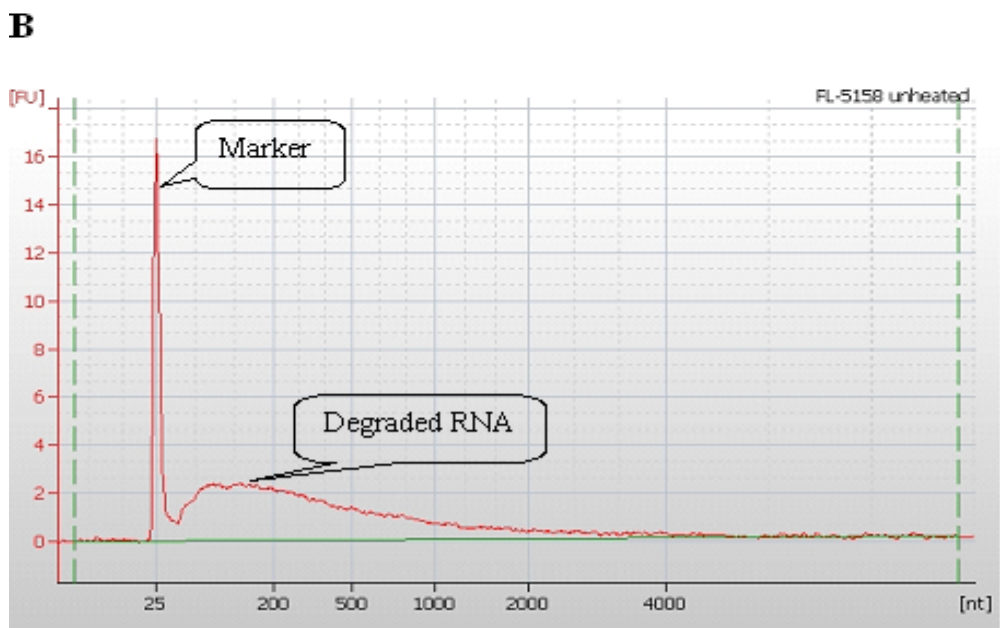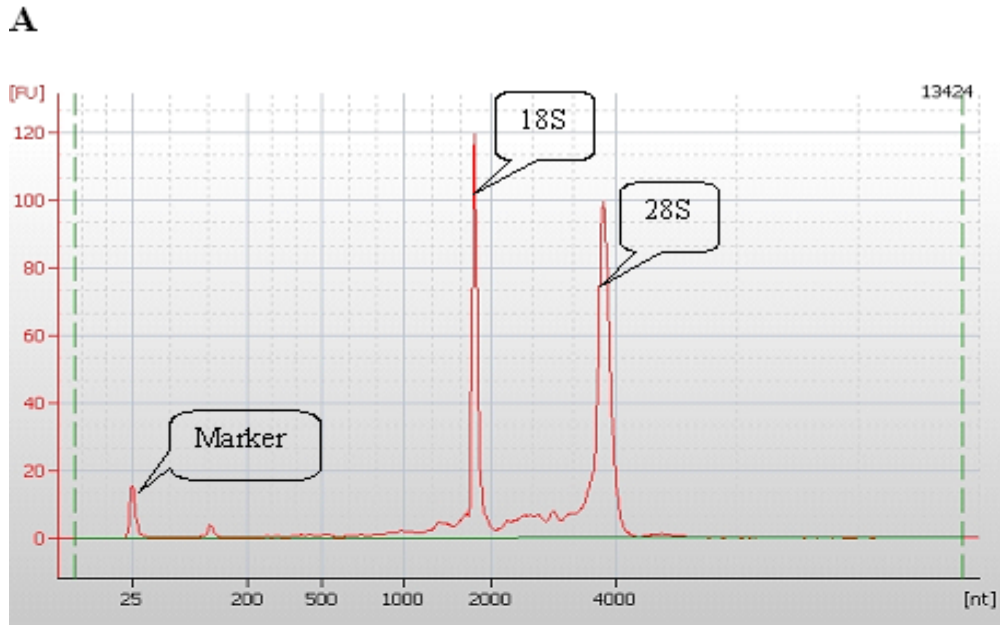
Figure 4-1. Effects of formalin fixation and paraffin embedding on RNA. (A) Frozen sample derived total RNA electrophorogram on Agilent Bioanalyzer Nanochip assay. (B) FFPE derived total RNA electrophorogram on Agilent Bioanalzyer Nanochip assay. The discrete 18S and 28S ribosomal RNA peaks indicate the high quality of RNA in the frozen sample. The FFPE sample derived RNA lacks the ribosomal peaks, indicating overall degradation of RNA.
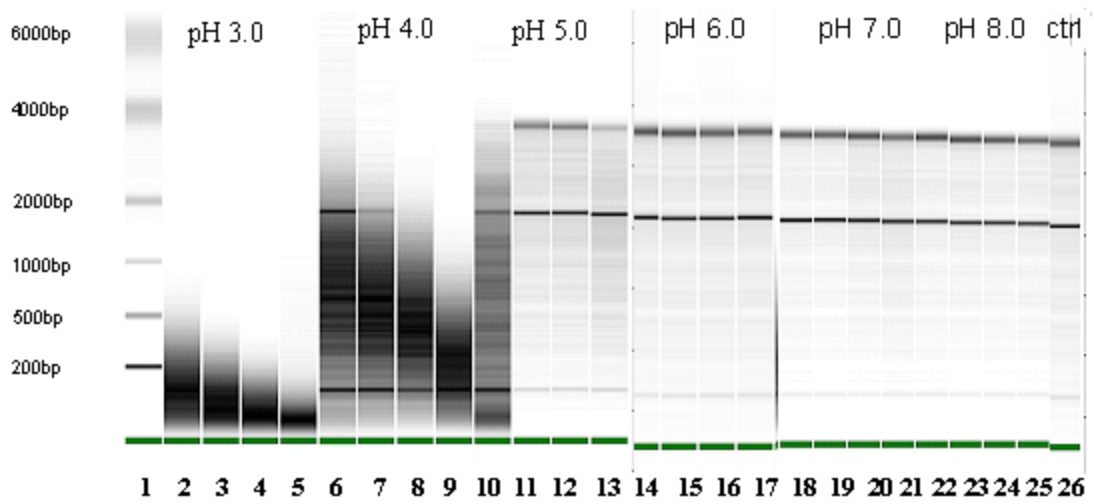
Figure 4-2 Effects of heat treatment at different pH on RNA integrity. Lane 1, RNA ladder; Lane2-5, RNA treated at pH 3.0; Lane 6-9, RNA treated at pH 4.0; Lane 10-13, RNA treated at pH 5.0; Lane 14-17, RNA treated at pH 6.0; Lane 18-21, RNA treated at pH 7.0; Lane 22-25, RNA treated at pH 8.0. For RNA treated at the same pH, the treated temperature are 60° C, 65° C, 70° C, 75° C from left to right.
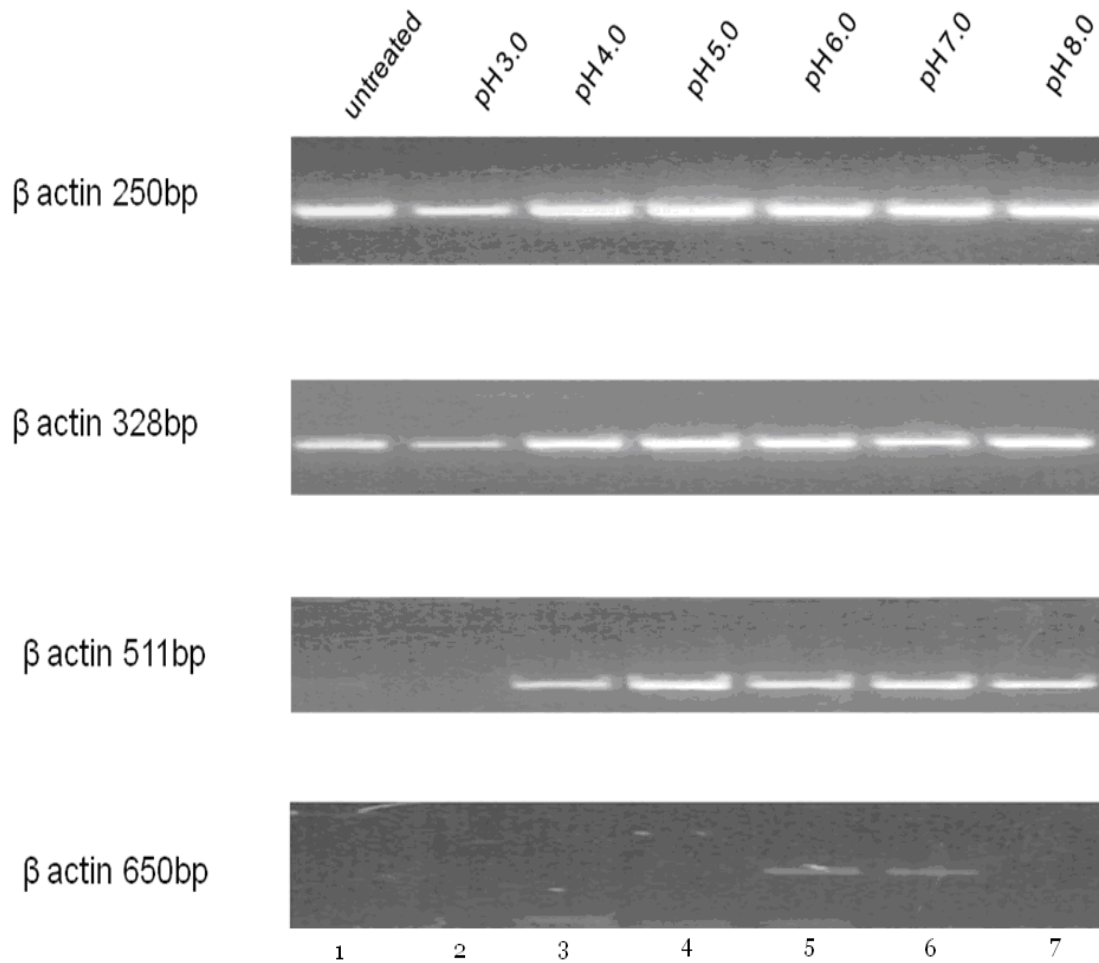
Figure 4-3 Effects of pH on RT-PCR amplification of RNA. FFPE sample-derived RNA was treated at various pH (3-8) at 75 °C for 30 minutes, then used to amplify different size of β-actin fragments. Lane 1, untreated RNA control; lane 2, RNA treated at pH 3; lane 3, RNA treated at pH 4; lane 4, RAN treated at pH 5; lane 5, RNA treated at pH 6; lane 6, RNA treated at pH 7; lane 7, RNA treated at pH 8.
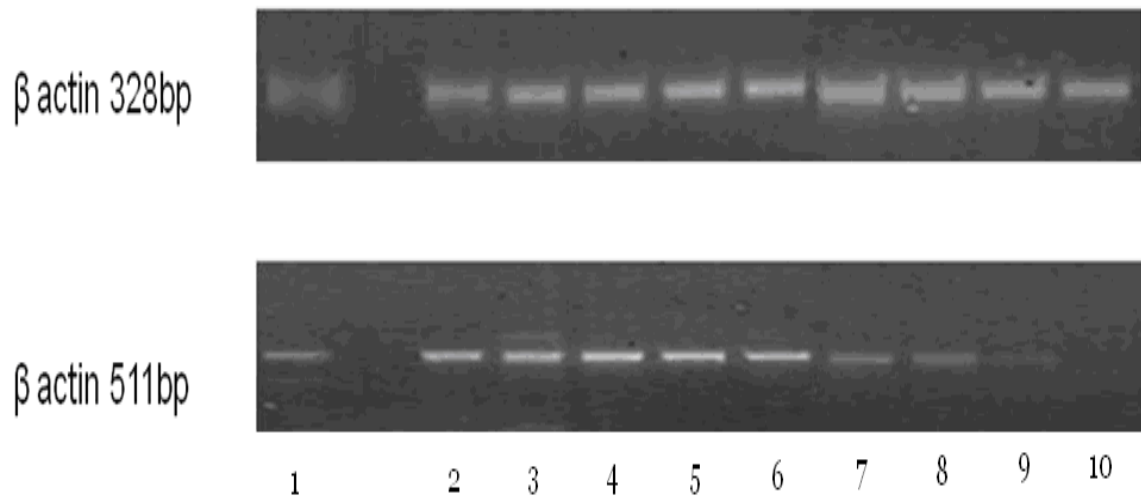
Figure 4-4   Effects of temperature on RT-PCR amplification FFPE sample-derived RNA was treated at various temperatures (60°C-100°C) for 60 minutes, then used to amplify different size of β-actin fragments. Lane 1, untreated RNA control; lane 2, RNA treated at 60°C; lane 3, RNA treated at 70°C; lane 4, RNA treated at 75°C; lane 5, RNA treated at 80°C; lane 6, RNA treated at 84°C; lane 7, RNA treated at 86°C; lane 8, RNA treated at 90°C; lane 9, RNA treated at 96°C; lane 10, RNA treated at 100°C

	Sample 05-19322	Sample 05-10508	Sample 05-13381	Sample 05-13947
Frozen (Tfr)	583	260	228	228
Untreated FFPE(Tu)	402	181	241	277
80 ° C treated FFPE (T80tr)	462	244	265	197
86 ° C treated FFPE (T86tr)	589	396	290	410
Number of features for analysis	13321	13649	13167	12682

Table 4-1 Background noise thresholds (in pixels) for each array based on individual histograms of the data to exclude features that cluster on the low end of the histogram. The number of features for the analysis after removal of low intensity and saturated features is shown.

	86 °C enhanced feature number	80 °C enhanced feature number	80°C&86°C enhanced feature number	Expected features number enhanced @80&86 by chance
Sample 05-19322 (N=13321)	4600(34.5%)	5137(38.6%)	3462(26.0%)	1774*
Sample 05-10508 (N=13649)	6358(46.6%)	10462(76.7%)	6056(44.4%)	4873*
Sample 05-13381 (N=13167)	2657(20.2%)	3659(27.8%)	2065(15.7%)	738 *
Sample 05-13947 (N=12682)	785(6.2%)	8608(67.9%)	711(5.6%)	533*

* Number of expected features to be enhanced is significantly lower than observed with a P value less than 0.01

Table 4-2 Number of features enhanced by treatment analysis on mRNA array platform.

Sample ID	Number of extreme features compared	Mean intensity of most enhanced features	Mean intensity of most decreased features	Students t test p value
05-19322	N=10	17720	7554	0.012
	N=100	17597	11245	0.000*
	N=500	13249	10410	0.000*
	N=1000	10774	9388	0.000*
05-10508	N=10	42588	26072	0.009
	N=100	30441	11554	0.000*
	N=500	19938	3674	0.000*
	N=1000	16510	2643	0.000*
05-13381	N=10	45710	21649	0.001
	N=100	40521	18801	0.000*
	N=500	31159	10536	0.000*
	N=1000	23553	7074	0.000*
05-13947	N=10	18212	6536	0.000*
	N=100	14109	5031	0.000*
	N=500	10053	3642	0.000*
	N=1000	6495	3209	0.000*

Table 4-3 t test comparing feature intensity between most enhanced features and most decreased features after 80° C treatment on mRNA array platform. For each pair of matched frozen and FFPE samples, equal number (N) of most enhanced features were compared to most decreased features (N=10,100,500,1000). t test showed enhanced features have a significant higher intensity, indicating the abundance of the template.

*Whenever p value was less than 0.0001, SPSS gives out p value of 0.000.

Sample ID	Number of extreme features compared	Mean GC content % of most enhanced features	Mean of GC content % of most decreased features	Students t test p value
05-19322	N=10	47.3	55.5	0.059
	N=100	48.5	57.8	0.000*
	N=500	48.6	55.8	0.000*
	N=1000	48.6	54.0	0.000*
05-10508	N=10	48.5	42.0	0.038
	N=100	48.4	46.6	0.094
	N=500	46.3	47.3	0.038
	N=1000	45.8	47.3	0.000*
05-13381	N=10	47.8	52.3	0.253
	N=100	46.1	50.0	0.000*
	N=500	46.2	49.7	0.000*
	N=1000	46.5	52.0	0.000*
05-13947	N=10	63.0	65.7	0.654
	N=100	51.7	65.7	0.000*
	N=500	50.6	59.8	0.000*
	N=1000	49.1	57.2	0.000*

Table 4-4 t test comparing probe GC content between most enhanced features and most decreased features after 80° C treatment on mRNA array platform. For each pair of matched frozen and FFPE samples, equal number (N) of most enhanced features were compared to most decreased features (N=10,100,500,1000). t test failed to show any relationship between probe GC content and enhancement status.

*Whenever p value was less than 0.0001, SPSS gives out p value of 0.000.

	Sample 05-19322		Sample 05-10508			Sample 05-13381			Sample 05-13947		
	Frozen vs. FFPE untr	Frozen vs. FFPE 80 tr	Frozen vs. FFPE 86 tr	Frozen vs. FFPE untr	Frozen vs. FFPE 80 tr	Frozen vs. FFPE 86 tr	Frozen vs. FFPE untr	Frozen vs. FFPE 80 tr	Frozen vs. FFPE 86 tr	Frozen vs. FFPE untr	Frozen vs. FFPE 80 tr	Frozen vs. FFPE 86 tr
Spearman Rank Coefficient	0.712	0.709	0.694	0.680	0.806	0.770	0.522	0.722	0.735	0.789	0.806	0.772
Correlation change after treatment	<0.1 change			~0.12 increase			~0.2 increase			<0.1 change		

Table 4-5 mRNA profile correlation changes after heat treatment

CHAPTER 5 Discussion and Conclusions

Gene expression based studies, coupled with genomic and proteomic level investigations, are providing opportunities for better understanding of various diseases at the molecular level, leading to discoveries of potential biomarkers and therapeutic targets [8] [9] [10] [11]. To achieve these goals, large scale gene expression analysis needs to be performed in a robust and reliable way. However, fresh or snap frozen samples, which are regarded as the best tissue source for gene expression analyses, are limited. On the other hand, the more broadly available FFPE samples with their detailed clinical annotation have not been systematically investigated with respect to the quality of various RNA species and to what extend can these RNAs be used reliably for gene expression analyses.

Using matched snap frozen and FFPE human tissue samples obtained from the clinical setting, our study directly addressed these questions by comparing gene expression profiles generated from matched clinical tissue samples.

5.1 Global profiling FFPE derived-miRNA

miRNAs serve as a good starting point in this project. Previously, good correlations were found between matched frozen and FFPE miRNA profiles using either RNA-primed, array-based Klenow enzyme (RAKE) microarray platform [69], or locked nucleic acid (LNA) based miRNA arrays[70]. Compared to mRNAs, miRNAs have better chances to survive FFPE processing without being significantly fragmented and chemically modified because: 1) In cytoplasm, mature miRNA is incorporated into the RISC ribonucleoprotein complex [26], where protein spatial hindrance may render it less liable to RNase fragmentation. In addition, the longer half life of mature miRNA molecules

(several hours to days) makes them inherently less affected by delayed fixation [73] [74] [75] [76] [77]. 2) Mature miRNA has no poly A tail and is much smaller in size (~18-24 nt) than most mRNAs; thus fewer hydroxymethyl groups are added during formalin fixation. According to base modification rates in Masuda's study [45], for a 24 nt miRNA with 6 of each type of ribonucleotide, approximate two adenines and two cytosines will be modified and subsequently crosslinked with other macromolecules, while modification and crosslinking effects are almost negligible for guanine and uracil. 3) When FFPE tissue sections are incubated in proteinase K solution at moderate temperature for miRNA extraction, the heat may provide enough energy to reverse the limited number of base modifications and break cross linking structures found associated with these small molecules.

Capillary electrophorograms of frozen sample derived total RNA showed a clear miRNA species peak. In contrast, capillary electrophoresis of total RNA isolated from FFPE samples showed a hump towards low molecular weight (Figure 3-1) due to degradation of larger RNA molecules (rRNA, tRNA and mRNA), making it difficult to assess the miRNA quality. Traditional RNA quality evaluation approaches, such as 28S/18S ratio or more sophisticated RNA integrity number (RIN) by Agilent Bioanalyzer, provided little information regarding miRNA quality in this situation, because the larger RNA species, ribosomal RNA in particular, are given more weight in both algorithms to estimate total RNA quality [78]. A universal RNA quality estimation based on large RNA molecules may not give an appropriate estimation of miRNA quality in FFPE samples. Therefore, miRNA specific quality control approaches need to be developed for precise quality

estimation prior to molecular assays. A PCR based approach, similar to that of measuring 3'/5' ratio of mRNA, might be the basis for such assay. For instance, after a miRNA being reverse transcribed into cDNA, a common reverse primer, with a primer targeting 5' end of the miRNA or a primer targeting 3' end of the miRNA can be used to amplify target miRNA. Intact miRNA will give out a 3'/5' ratio close to 1, and an increase ratio would indicate miRNA fragmentation.

In this study, miRNA profiles of matched frozen and FFPE samples were compared using the Agilent miRNA array platform which has several advantages: 1) The 3' end labeling method used for this platform is tolerant to nucleotide damage in substrate miRNAs as long as the 3' end of target molecule remains intact. 2) Highly specific probe sequences effectively distinguish targeted miRNAs from unintended mRNAs, making miRNA enrichment unnecessary [79] and resulting in more accurate miRNA hybridization patterns. 3) This platform has been shown to measure precisely input miRNA from 0.2 amol to 2 fmol [79], a range covering both high and low expression miRNAs. 4) Only 100ng total RNA is required to generate miRNAs expression profiles, compared to microgram total RNA input required on other platform. The robustness of this platform is further shown by high reproducibility of extraction, labeling and hybridization processes in our data (Fig 3-3, Fig 3-4, Fig 3-5). The slightly lower correlation observed in Figure 3-5 reflects the combination of variation occurring during extraction, labeling and hybridization in addition to slide to slide variation, so it would be safe to assume that slide to slide variation alone does not greatly skew the final profile.

In our hands, it is technically feasible to profile miRNA isolated from archival FFPE samples on the Agilent miRNA array platform using protocols designed for frozen sample profiling. FFPE samples with a maximum storage time of two years were successfully profiled and yielded similar signal levels to matched frozen samples. Whether older archival samples can be profiled successfully remains to be seen. Our data demonstrated that 99.6% of miRNAs (468 out of 470) in FFPE samples had no greater than 1 fold signal shift compared to those in frozen samples, higher than results from Li et al's study where only 65.58% miRNAs (101 out of 154) displayed less than 1 fold change on qRT-PCR platform [80]. The difference may simply due to the higher sensitivity of the q PCR platform, which is capable of detecting low fold changes better than the microarray platform(most outliers identified on qRT-PCR platform have a less than 4 fold signal change). We recognize the lack of solid evidence supporting the use of Z score transformation for interarray normalization when miRNA profiles between frozen and FFPE samples are compared. The only available and supportive evidence is the relative stability of majority of 160miRNAs after FFPE processing on qRT-PCR platform [80], further miRNA profiling on various platforms will clarify this issue.

Consistent high correlations between matched frozen and FFPE samples suggest that miRNA profiling on FFPE samples may provide accurate reflection of what would be observed in fresh/snap frozen tissue, which agrees with previous data [70] [79] [81]. Both Kendall tau and Spearman rank correlation coefficient results between matched frozen and FFPE samples were significantly higher than would be expected by chance (near zero and no significance of correlation), which was simulated by reshuffling two data sets

from matched samples independently and randomly and recalculating the Kendall tau and Spearman rank correlation coefficient. In our hands, the worst Spearman rank correlation coefficient between matched clinical samples was 0.847, slightly lower than a minimum r of 0.927 when in-lab made FFPE samples were compared to matched frozen samples on LNA based miRNA array platform [70]. Assuming the difference comes solely from variations of FFPE sample preparation, this slight correlation decrease when archival clinical FFPE samples are compared to frozen samples shows strong evidence that miRNAs are less affected than mRNAs by delayed fixation and storage time. The similarity of matched samples was further confirmed in the line plots (Fig 3-6), where FFPE-derived miRNAs retained most of the characteristic expression pattern of the frozen counterpart. It is also worth noting that in cases where the FFPE-derived miRNA deviated from the frozen sample profile, no fixed pattern was found. Multiple factors may contribute to this signal intensity deviation, such as miRNAs degradation & miRNA modification by FFPE processing or stress induced miRNA expression increase, these non biological noises due to FFPE preparation may pose some challenges for data analysis. It remains to be seen how downstream applications such as identifying differentially expressed miRNAs, tumor classification, will be affected by these FFPE induced noises.

5.2 FFPE derived mRNA global profiling

Several recent studies reported successful profiling of FFPE sample-derived mRNAs and gene expression profiles that could correctly identify tumor type, origin of tumor and certain pathways [67] [68]. However, profiling mRNAs isolated from unselected archival

FFPE samples on a standard microarray platform remains difficult. Intact poly A tails of mRNAs and long mRNA fragments are essential for T7 based linear amplification and subsequent profiling on most array platforms. As a result, a huge amount of gene expression information is lost or distorted when highly degraded mRNAs are profiled [70]. Our data further confirmed this conclusion, as one matched pair of frozen and FFPE samples (sample 05-19322) was profiled both on mRNA arrays and miRNA arrays. In contrast to the good correlations of the miRNA profiles (Kendall tau=0.758-0.783, Spearman rank correlation coefficient=0.913-0.93), the matched mRNA profiles showed substantially lower correlations (Kendall tau=0.550, Spearman rank correlation coefficient=0.712), which agrees with results from Xi et al's study [70], indicating mRNA are more liable than miRNA during FFPE processing.

Several potential strategies were available to improve the quality of mRNAs isolated from FFPE samples for downstream gene expression profiling. Extending proteinase K digestion up to 20 hours at 60° C has been reported to improve mRNAs quality for downstream RT-PCR, and a moderate correlation (0.65, 0.78) between paired frozen and FFPE samples were found when such FFPE sample-derived mRNA were profiled [55]. In our hands, longer proteinase K digestion did yield more RNA (~30μg) compared to RNA extraction protocols with shorter digestion time (< 8 hours) (<10μg). However, the quality improvement on RT-PCR platform could be described as marginal at most (data not shown). So far, there has been no systematic study comparing various FFPE sample RNA extraction protocols on array platform, as a result, it remains unclear whether RNA isolation protocol with extended proteinase K digestion would produce mRNAs with

better quality for profiling. However, since a global correlation of 0.7 or even higher between matched frozen and FFPE samples has also been reported when shorter proteinase K digestion is employed for RNA extraction [65] [66], claiming longer digestion would greatly improve the quality of mRNAs sounds questionable.

More recently, a creative new strategy has been developed to restore degraded mRNA sequence prior to T7 based *in vitro* transcription amplification and subsequent global profiling. Short single-stranded T7-oligo-dT24-VN cDNA sequence, which is obtained from FFPE sample derived RNA was used as primers for the reverse transcription of complementary RNA templates contained in a sense-RNA library generated from human reference RNA. It has been shown that this restoration strategy before T7 based *in vitro* transcription significantly increased the signal on microarray platform while greatly reducing the non specific signal. A 35%-41% restoration of the transcripts from 10 year old archived FFPE samples has been reported in the study [82]. However, since this approach also relies on the existence of poly A tails of mRNAs for cDNA synthesis, and sample manipulation is complex, so it was not tried here.

In this project, we attempted a simple post extraction heat treatment to improve mRNA quality. Our data showed that heating FFPE sample-derived RNA increased the maximum amplicon size of β-actin derived from the RT-PCR, in agreement with previous data [45] [57]. However, there was significant difference regarding the level of improvement. In our hands, a maximum 150bp increase of amplicon size was observed, similar to less than 100bp increases in Kiyohiro's study [57]. Both improvements are significantly smaller than the greater than 1000bp increase in Masuda's study [45]. The

nature of the FFPE samples used in studies may explain this huge gap: in Masuda's study, FFPE samples were made under optimal conditions to avoid RNA fragmentation, such as minimizing fixation delay, fixing at low temperature and extracting RNA without long storage times. Because RNA modification and cross linking appears to be the major determinants dictating whether a given amplicon can be successfully amplified [50], it is not surprising that reversing base modification and cross linking alone by heat treatment would bring more than 1000bp improvement on RT-PCR platform when carefully prepared samples are used. On the contrary, in Kiyohiros study [57] and our experiments, routinely processed FFPE samples with an age of more than one year old were used. In this case, the maximum product amplifiable on RT-PCR is mainly limited by the maximum size of target amplicon within total RNA, which is often less than 600bp due to fixation delay and continuous fragmentation occurred at storage [50]. This smaller RNA quality improvement on archival FFPE samples may suggest the limited benefit of a heat treatment on samples obtained from the clinical setting.

Previously, an optimal heat treatment in pH 4 buffers at 70° C for 45 minutes was suggested by Kiyohiro's group[57]. However, our data indicated that treating RNA in a near neutral buffer (pH 6.0-8.0) produced the most prominent amplicon size increase following RT-PCR. In our hands, treatment in acidic condition (pH 3.0-5.0) had negative effects on 18s and 28s ribosomal RNA of intact RNA, and therefore presumably on mRNAs as well [83]. This was confirmed by our data where treatment in acidic conditions (pH 3.0) showed negative effects on mRNA following RT-PCR (Fig 4-3). Likewise, our optimal temperature ranges from 60° C to about 84° C, differed from the

previously suggested single optimal temperature of 70°C [45] [57]. Because different FFPE samples and genes were used in these studies, it would be impossible to determine which condition is optimal and provides most benefits. Considering individual mRNA fragments, it is very likely that optimal conditions are sequence specific, and a universal optimal treatment condition for all genes may not exist at all. It is worth noting that extraction protocols may be crucial to determine how well a post extraction heat treatment may reverse the base modification and cross linking. A longer proteinase K digestion at higher temperature may complete reversion to its upper limit at the extraction step, and no further mRNA quality improvement would be achieved via an additional post extraction heat treatment. For example, it has been shown on RT-PCR platform that heating RNA isolated with a proteinase K digestion of 20 hours at 60°C didn't improve RNA quality [55]. Therefore, to avoid possible mRNA damage, we recommend that post extraction heat treatment shouldn't be performed if RNA is isolated using protocols with long proteinase K digestion at high temperature, although the definition of long digestion at high temperature remains obscure.

To assess the genome wide effects of a single heat treatment, we compared the profiles generated from matched frozen and unheated or heated FFPE samples. This direct comparison provided a straightforward way to assess the effects of the treatment on mRNAs individually and globally. To our knowledge, this is the first time the effects of heat treatment on performance on an array platform have been investigated, although moderate post extraction heat treatment has been empirically employed in several profiling protocols such as the Paradise system [66].

Initially, the Agilent low RNA input amplification kit (Agilent, Santa Clara, CA), whose protocol employs a T7 based one round *in vitro* transcription, was used to amplify FFPE sample derived mRNA. Unfortunately, most reactions failed to produce enough cRNA for downstream hybridization and dye incorporation efficiency was too low for profiling (data not shown) due to the poor quality of mRNA. To address this problem, we replaced the original primer, comprised of a T7 promoter sequence and a poly dT sequence, with a new hybrid primer comprised of a T7 promoter sequence and a random hexamer. This approach significantly improved the yield of cRNA and dye incorporation efficiency (data not shown). However, the resulting profiles were poorly correlated to the profile generated from matched frozen sample. An appropriate ratio of random primer and dT primer mixture may be essential for linear amplification of all mRNA trancripts, as pointed by NuGene, the company which recently marketed a dT and random priming based amplification kit for profiling FFPE sample on Affymetrix array platform.

For most features in two of the samples (98.6% in sample 05-19322 and 78% in sample 05-10508), the frozen sample RNA had raw intensity values at least 50 pixels higher than the FFPE untreated sample, which is in agreement with expected intensity decrease for almost all features due to FFPE processing. However, for two other samples, less than half of the features(43.2% in sample 05-13381 and 21.0% in sample 05-13947) showed at least 50 pixels higher raw intensity when frozen samples were compared to FFPE untreated samples. Why should it be so is not clear. We proposed that several factors may account for this contradictory observation: First, because of a lack of a proper interarray normalization method, some of the differences may be masked by variations introduced

by microarray manipulations, which is particularly relevant for most low abundance transcripts. Secondly, non specific hybridization due to RNA fragmentation may increase the raw intensity on the FFPE sample derived array, reducing or even offsetting the signal difference between frozen samples and matched untreated FFPE samples.

In agreement with previous postulations that a single heat treatment may have different or even opposite effects on various transcripts and sequences, comparison of intensities between untreated(N=4) and treated FFPE samples(N=4) showed feature and sequence dependant effects. 6.2% - 76.7% of features were enhanced after the treatment (feature raw intensity values of treated samples at least 50 pixels higher than untreated sample). Obviously, arbitrary cutoff values defining a feature being enhanced would influence number of enhanced features being counted, a potential limitation for future comparison of same kind of studies on different array platforms. The percentage of features enhanced varied greatly under different treatment temperatures and in different samples, which may be attributable to several factors: enhancement may occur in a treatment condition and sample dependant manner, in addition, lacking interarray normalization and noise signal due to non specific hybridization may mask or exaggerate the signal difference.

A random heat-induced enhancement would have little potential for practical application. Since none of the treated FFPE-derived RNA was profiled in duplicate in our study, it was impossible to exclude the existence of random enhancement. However, our data are sufficient to answer the question of whether features were enhanced totally by chance within the same sample. Irrelevant of cutoff values defining a feature as being enhanced, results showed estimated numbers to be enhanced were significantly smaller than

observed enhanced numbers with a p value less than 0.01 in all four samples tested, indicating features were probably enhanced more than by mere chance.

Further analysis suggested that abundant transcripts may be more likely to benefit from heat treatment, while the same heat treatment may cause negative effects on less abundant transcripts. This was supported by the observation that most of the enhanced features in our study had greater intensity value in the frozen samples compared to decreased features. This may explain why higher temperatures were indicated as optimal in our hands when an abundant house keeping gene (β-actin) was used for optimization by RT-PCR. Theoretically, the GC content of a given transcript may also be essential in determining the effect of a heat treatment, because a higher GC content could indicate less base modification and cross linking based on Masuda's study [45]. Because we profiled heterogeneous mRNAs in our study, the exact sequence and GC content of mRNAs hybridizing to each probe were unknown. As a result, it was impossible to compare the GC content of targets corresponding to enhanced and decreased features. A preliminary analysis was performed to compare the GC content of the probes corresponding to the most enhanced features and most decreased features. This failed to show any distinctive relationship between GC content and enhancement status. However, this is not totally unexpected, as GC content of a given mRNA template and corresponding probe on array may differ greatly. Further studies using homogeneous mRNA samples may be helpful to clarify this issue. For example, FFPE processed synthetic oligonucleotide with serial known GC content could be heated and then

quantified on qRT-PCR platform, and the Ct value shift used to indicate the direction and the level of effects by heat treatment.

Finally, the genome wide effect of a post extraction heat treatment was evaluated. In our hands, even one hour at 86° C didn't decrease correlation significantly, suggesting a prolonged post extraction heat treatment probably causes little global mRNA quality damage. Two possible reasons may account for this observation. First, almost all heat sensitive mRNA populations may have already been damaged during FFPE processing, with little further damage done by a post extraction heat treatment. Secondly, beneficiary effects of heat treatment by reversing base modification and cross linking may offset or surpass any negative effects caused by heat treatment, resulting in a global mRNA quality improvement. On the other hand, changes to correlations between FFPE and frozen pairs clearly showed a sample dependant effect, suggesting limited benefits of the heat treatment. No relationship was found between a correlation improvement and percentage of features enhanced. Although increased global correlation in a few samples may have reflected a better match between the frozen and treated FFPE pairs, indicating a possible global mRNA quality improvement, the underlying biochemistry is complex, and it remains to be seen whether such global correlation improvement suggests more reliable gene expression data from those treated FFPE samples. It is interesting to note in our data that samples with relative poor correlations prior to treatment (Spearman rank correlation coefficient<0.7 between frozen and FFPE untreated samples) showed greater correlation improvement after heat treatment, while samples with relatively good correlations prior to treatment (Spearman rank correlation coefficient >0.7 between frozen and FFPE

untreated samples) had almost negligible correlation changes after heat treatment. This is in agreement with previous data from our lab (unpublished). We postulate that correlation between frozen and FFPE untreated samples may reflect the level of base modification and cross linking in a FFPE sample. A poorer correlation indicates more severe mRNA modification; as a result more benefit can be achieved from a post extraction heat treatment and subsequent correlation improvement.

Further in depth studies are needed to achieve a comprehensive picture of which RNA templates may benefit from a given heat treatment and how to maximize that benefit to improve mRNA quality for gene expression analyses on archival samples.

5.3 Conclusions

In summary, we conclude that FFPE samples may retain miRNA populations well enough for routine profiling, although it remains unclear how FFPE processing would influence the expression information on individual miRNA molecules. In the case of mRNA, profiling unselected FFPE samples on a standard microarray platform is still challenging and error prone, although technical advances in microarray design may break this barrier in the near future.

References:

1. Taegtmeyer H. Genetics of energetics: transcriptional responses in cardiac metabolism. Ann Biomed Eng 2000; Aug;28(8):871-6.

2. Yan C, Miller CL, Abe J. Regulation of phosphodiesterase 3 and inducible cAMP early repressor in the heart. Circ Res 2007; Mar 2;100(4):489-501.

3. Case CC. Transcriptional tools for aging research. Mech Ageing Dev 2003; Jan;124(1):103-8.

4. Lehrmann E, Colantuoni C, Deep-Soboslay A, Becker KG, Lowe R, Huestis MA, Hyde TM, Kleinman JE, Freed WJ. Transcriptional changes common to human cocaine, cannabis and phencyclidine abuse. PLoS ONE 2006; Dec 27;1:e114.

5. Thomas GR, Nadiminti H, Regalado J. Molecular predictors of clinical outcome in patients with head and neck squamous cell carcinoma. Int J Exp Pathol 2005; Dec;86(6):347-63.

6. Lossos IS, Morgensztern D. Prognostic biomarkers in diffuse large B-cell lymphoma. J Clin Oncol 2006; Feb 20;24(6):995-1007.

7. Marshall T, Williams KM. Proteomics and its impact upon biomedical science. Br J Biomed Sci 2002;59(1):47-64.

8. Lewis RS, Ward AC. Stat5 as a diagnostic marker for leukemia. Expert Rev Mol Diagn 2008; Jan;8(1):73-82.

9. Carella AM, Lerma E. Imatinib mesylate in chronic myeloid leukemia. Curr Stem Cell Res Ther 2007; Sep;2(3):249-51.

10. Jabbour E, Cortes JE, Ghanem H, O'Brien S, Kantarjian HM. Targeted therapy in chronic myeloid leukemia. Expert Rev Anticancer Ther 2008; Jan;8(1):99-110.

11. Pal SK, Pegram M. HER2 targeted therapy in breast cancer...beyond Herceptin. Rev Endocr Metab Disord 2007; Sep;8(3):269-77.

12. LeBrun D, Baetz T, Foster C, Farmer P, Sidhu R, Guo H, Harrison K, Somogyi R, Greller LD, Feilotter H. Predicting outcome in follicular lymphoma by using interactive gene pairs. Clin Cancer Res 2008; Jan 15;14(2):478-87.

13. Dhanasekaran SM, Barrette TR, Ghosh D, Shah R, Varambally S, Kurachi K, Pienta KJ, Rubin MA, Chinnaiyan AM. Delineation of prognostic biomarkers in prostate cancer. Nature 2001; Aug 23;412(6849):822-6.

14. Martoglio AM, Tom BD, Starkey M, Corps AN, Charnock-Jones DS, Smith SK. Changes in tumorigenesis- and angiogenesis-related gene transcript abundance profiles in ovarian cancer detected by tailored high density cDNA arrays. Mol Med 2000; Sep;6(9):750-65.

15. Hong TM, Yang PC, Peck K, Chen JJ, Yang SC, Chen YC, Wu CW. Profiling the downstream genes of tumor suppressor PTEN in lung cancer cells by complementary DNA microarray. Am J Respir Cell Mol Biol 2000; Sep;23(3):355-63.

71

16. Xu J, Stolk JA, Zhang X, Silva SJ, Houghton RL, Matsumura M, Vedvick TS, Leslie KB, Badaro R, Reed SG. Identification of differentially expressed genes in human prostate cancer using subtraction and microarray. Cancer Res 2000; Mar 15;60(6):1677-82.

17. Clark EA, Golub TR, Lander ES, Hynes RO. Genomic analysis of metastasis reveals an essential role for RhoC. Nature 2000; Aug 3;406(6795):532-5.

18. van de Vijver MJ, He YD, van't Veer LJ, Dai H, Hart AA, Voskuil DW, Schreiber GJ, Peterse JL, Roberts C, Marton MJ, Parrish M, Atsma D, Witteveen A, Glas A, Delahaye L, van der Velde T, Bartelink H, Rodenhuis S, Rutgers ET, Friend SH, Bernards R. A gene-expression signature as a predictor of survival in breast cancer. N Engl J Med 2002; Dec 19;347(25):1999-2009.

19 van 't Veer LJ, Dai H, van de Vijver MJ, He YD, Hart AA, Mao M, Peterse HL, van der Kooy K, Marton MJ, Witteveen AT, Schreiber GJ, Kerkhoven RM, Roberts C, Linsley PS, Bernards R, Friend SH. Gene expression profiling predicts clinical outcome of breast cancer. Nature 2002; Jan 31;415(6871):530-6.

20. Buyse M, Loi S, van't Veer L, Viale G, Delorenzi M, Glas AM, d'Assignies MS, Bergh J, Lidereau R, Ellis P, Harris A, Bogaerts J, Therasse P, Floore A, Amakrane M, Piette F, Rutgers E, Sotiriou C, Cardoso F, Piccart MJ; TRANSBIG Consortium. Validation and clinical utility of a 70-gene prognostic signature for women with node-negative breast cancer. J Natl Cancer Inst 2006; Sep 6;98(17):1183-92.

21. Meyer S, Temme C, Wahle E. Messenger RNA turnover in eukaryotes: pathways and enzymes. Crit Rev Biochem Mol Biol 2004; Jul-Aug;39(4):197-216.

22. Bohnsack MT, Czaplinski K, Gorlich D. Exportin 5 is a RanGTP-dependent dsRNA-binding protein that mediates nuclear export of pre-miRNAs. RNA 2004; Feb;10(2):185-91.

23. Lee Y, Jeon K, Lee JT, Kim S, Kim VN. MicroRNA maturation: stepwise processing and subcellular localization. EMBO J 2002; Sep 2;21(17):4663-70.

24. Brennecke J, Cohen SM. Towards a complete description of the microRNA complement of animal genomes. Genome Biol 2003;4(9):228.

25. Pillai RS. MicroRNA function: multiple mechanisms for a tiny RNA?. RNA 2005; Dec;11(12):1753-61.

26. Jay C, Nemunaitis J, Chen P, Fulgham P, Tong AW. miRNA profiling for diagnosis and prognosis of human cancer. DNA Cell Biol 2007; May;26(5):293-300.

27. Olsen M, Madsen HO, Hjalgrim H, Ford A, Schmiegelow K. Stability of cord blood RNA measured by house keeping transcripts: relevance for large-scale studies of childhood leukaemia. Leukemia 2006; Dec;20(12):2214-7.

28. Orphanides G, Reinberg D. A unified theory of gene expression. Cell 2002; Feb 22;108(4):439-51.

29. Medeiros F, Rigl CT, Anderson GG, Becker SH, Halling KC. Tissue handling for genome-wide expression analysis: a review of the issues, evidence, and opportunities. Arch Pathol Lab Med 2007; Dec;131(12):1805-16.

30. Garneau NL, Wilusz J, Wilusz CJ. The highways and byways of mRNA decay. Nat Rev Mol Cell Biol 2007; Feb;8(2):113-26.

31. Proudfoot N. Connecting transcription to messenger RNA processing. Trends Biochem Sci 2000; Jun;25(6):290-3.

32. Qu Y, Boutjdir M. RNase protection assay for quantifying gene expression levels. Methods Mol Biol 2007;366:145-58.

33. Distler JH, Distler O, Neidhart M, Gay S. Subtractive hybridization. Methods Mol Med 2007;135:77-90.

34. Porter D, Yao J, Polyak K. SAGE and related approaches for cancer target identification. Drug Discov Today 2006; Feb;11(3-4):110-8.

35. Bustin SA, Benes V, Nolan T, Pfaffl MW. Quantitative real-time RT-PCR--a perspective. J Mol Endocrinol 2005; Jun;34(3):597-601.

36. Wang TH, Chao A. Microarray analysis of gene expression of cancer to guide the use of chemotherapeutics. Taiwan J Obstet Gynecol 2007; Sep;46(3):222-9.

37. Kantarjian HM, Talpaz M, Cortes J, O'Brien S, Faderl S, Thomas D, Giles F, Rios MB, Shan J, Arlinghaus R. Quantitative polymerase chain reaction monitoring of BCR-ABL during therapy with imatinib mesylate (STI571; gleevec) in chronic-phase chronic myelogenous leukemia. Clin Cancer Res 2003; Jan;9(1):160-6.

38. Yang JH, Lai JP, Douglas SD, Metzger D, Zhu XH, Ho WZ. Real-time RT-PCR for quantitation of hepatitis C virus RNA. J Virol Methods 2002; Apr;102(1-2):119-28.

39. Casabianca A, Gori C, Orlandi C, Forbici F, Federico Perno C, Magnani M. Fast and sensitive quantitative detection of HIV DNA in whole blood leucocytes by SYBR green I real-time PCR assay. Mol Cell Probes 2007; Oct-Dec;21(5-6):368-78.

40. Pentheroudakis G, Briasoulis E, Pavlidis N. Cancer of unknown primary site: missing primary or missing biology?. Oncologist 2007; Apr;12(4):418-25.

41. Blow N. Tissue preparation: Tissue issues. Nature 2007; Aug 23;448(7156):959-63.

42. Fox CH, Johnson FB, Whiting J, Roller PP. Formaldehyde fixation. J Histochem Cytochem 1985; Aug;33(8):845-53.

43. Godfrey TE, Kim SH, Chavira M, Ruff DW, Warren RS, Gray JW, Jensen RH. Quantitative mRNA expression analysis from formalin-fixed, paraffin-embedded tissues using 5' nuclease quantitative reverse transcription-polymerase chain reaction. J Mol Diagn 2000; May;2(2):84-91.

44. Abrahamsen HN, Steiniche T, Nexo E, Hamilton-Dutoit SJ, Sorensen BS. Towards quantitative mRNA analysis in paraffin-embedded tissues using real-time reverse transcriptase-polymerase chain reaction: a methodological study on lymph nodes from melanoma patients. J Mol Diagn 2003; Feb;5(1):34-41.

45. Masuda N, Ohnishi T, Kawamoto S, Monden M, Okubo K. Analysis of chemical modification of RNA from formalin-fixed samples and optimization of molecular biology applications for such samples. Nucleic Acids Res 1999; Nov 15;27(22):4436-43.

46. Rait VK, Zhang Q, Fabris D, Mason JT, O'Leary TJ. Conversions of formaldehyde-modified 2'-deoxyadenosine 5'-monophosphate in conditions modeling formalin-fixed tissue dehydration. J Histochem Cytochem 2006; Mar;54(3):301-10.

47. Loeb LA, Preston BD. Mutagenesis by apurinic/apyrimidinic sites. Annu Rev Genet 1986;20:201-30.

48. Douglas MP, Rogers SO. DNA damage caused by common cytological fixatives. Mutat Res 1998; Jun 5;401(1-2):77-88.

49. van Maldegem F, de Wit M, Morsink F, Musler A, Weegenaar J, van Noesel CJ. Effects of processing delay, formalin fixation, and immunohistochemistry on RNA Recovery From Formalin-fixed Paraffin-embedded Tissue Sections. Diagn Mol Pathol 2008; Mar;17(1):51-8.

50. von Ahlfen S, Missel A, Bendrat K, Schlumpberger M. Determinants of RNA quality from FFPE samples. PLoS ONE 2007; Dec 5;2(12):e1261.

51. Macabeo-Ong M, Ginzinger DG, Dekker N, McMillan A, Regezi JA, Wong DT, Jordan RC. Effect of duration of fixation on quantitative reverse transcription polymerase chain reaction analyses. Mod Pathol 2002; Sep;15(9):979-87.

52. Lewis F, Maughan NJ, Smith V, Hillan K, Quirke P. Unlocking the archive--gene expression in paraffin-embedded tissue. J Pathol 2001; Sep;195(1):66-71.

53. Coombs NJ, Gough AC, Primrose JN. Optimisation of DNA and RNA extraction from archival formalin-fixed tissue. Nucleic Acids Res 1999; Aug 15;27(16):e12.

54. Houze TA, Gustavsson B. Sonification as a means of enhancing the detection of gene expression levels from formalin-fixed, paraffin-embedded biopsies. BioTechniques 1996; Dec;21(6):1074,8, 1080, 1082.

55. Chen J, Byrne GE,Jr, Lossos IS. Optimization of RNA extraction from formalin-fixed, paraffin-embedded lymphoid tissues. Diagn Mol Pathol 2007; Jun;16(2):61-72.

56. Shi SR, Cote RJ, Taylor CR. Antigen retrieval techniques: current perspectives. J Histochem Cytochem 2001; Aug;49(8):931-7.

57. Hamatani K, Eguchi H, Takahashi K, Koyama K, Mukai M, Ito R, Taga M, Yasui W, Nakachi K. Improved RT-PCR amplification for molecular analyses with long-term preserved formalin-fixed, paraffin-embedded tissue specimens. J Histochem Cytochem 2006; Jul;54(7):773-80.

58. Rupp GM, Locker J. Purification and analysis of RNA from paraffin-embedded tissues. BioTechniques 1988; Jan;6(1):56-60.

59. Bhatnagar J, Guarner J, Paddock CD, Shieh WJ, Lanciotti RS, Marfin AA, Campbell GL, Zaki SR. Detection of West Nile virus in formalin-fixed, paraffin-embedded human tissues by

RT-PCR: a useful adjunct to conventional tissue-based diagnostic methods. J Clin Virol 2007; Feb;38(2):106-11.

60. Vogt S, Schneider-Stock R, Klauck S, Roessner A, Rocken C. Detection of hepatitis C virus RNA in formalin-fixed, paraffin-embedded thin-needle liver biopsy specimens. Am J Clin Pathol 2003; Oct;120(4):536-43.

61. Steele A, Uckan D, Steele P, Chamizo W, Washington K, Koutsonikolis A, Good RA. RT in situ PCR for the detection of mRNA transcripts of Fas-L in the immune-privileged placental environment. Cell Vis 1998; Jan-Feb;5(1):13-9.

62. Bao J, Li L, Wang Z, Barrett T, Suo L, Zhao W, Liu Y, Liu C, Li J. Development of one-step real-time RT-PCR assay for detection and quantitation of peste des petits ruminants virus. J Virol Methods 2008; Mar;148(1-2):232-6.

63. Koch I, Slotta-Huspenina J, Hollweck R, Anastasov N, Hofler H, Quintanilla-Martinez L, Fend F. Real-time quantitative RT-PCR shows variable, assay-dependent sensitivity to formalin fixation: implications for direct comparison of transcript levels in paraffin-embedded tissues. Diagn Mol Pathol 2006; Sep;15(3):149-56.

64. Antonov J, Goldstein DR, Oberli A, Baltzer A, Pirotta M, Fleischmann A, Altermatt HJ, Jaggi R. Reliable gene expression measurements from degraded RNA by quantitative real-time PCR depend on short amplicons and a proper normalization. Lab Invest 2005; Aug;85(8):1040-50.

65. Lee CH, Bang SH, Lee SK, Song KY, Lee IC. Gene expression profiling reveals sequential changes in gastric tubular adenoma and carcinoma in situ. World J Gastroenterol 2005; Apr 7;11(13):1937-45.

66. Coudry RA, Meireles SI, Stoyanova R, Cooper HS, Carpino A, Wang X, Engstrom PF, Clapper ML. Successful application of microarray technology to microdissected formalin-fixed, paraffin-embedded tissue. J Mol Diagn 2007; Feb;9(1):70-9.

67. Scicchitano MS, Dalmas DA, Bertiaux MA, Anderson SM, Turner LR, Thomas RA, Mirable R, Boyce RW. Preliminary comparison of quantity, quality, and microarray performance of RNA extracted from formalin-fixed, paraffin-embedded, and unfixed frozen tissue samples. J Histochem Cytochem 2006; Nov;54(11):1229-37.

68. Penland SK, Keku TO, Torrice C, He X, Krishnamurthy J, Hoadley KA, Woosley JT, Thomas NE, Perou CM, Sandler RS, Sharpless NE. RNA expression analysis of formalin-fixed paraffin-embedded tumors. Lab Invest 2007; Apr;87(4):383-91.

69. Nelson PT, Baldwin DA, Kloosterman WP, Kauppinen S, Plasterk RH, Mourelatos Z. RAKE and LNA-ISH reveal microRNA expression and localization in archival human brain. RNA 2006; Feb;12(2):187-91.

70. Xi Y, Nakajima G, Gavin E, Morris CG, Kudo K, Hayashi K, Ju J. Systematic analysis of microRNA expression of RNA extracted from fresh frozen and formalin-fixed paraffin-embedded samples. RNA 2007; Oct;13(10):1668-74.

79

71. Cheadle C, Vawter MP, Freed WJ, Becker KG. Analysis of microarray data using Z score transformation. J Mol Diagn 2003; May;5(2):73-81.

72. Yang YH, Dudoit S, Luu P, Lin DM, Peng V, Ngai J, Speed TP. Normalization for cDNA microarray data: a robust composite method addressing single and multiple slide systematic variation. Nucleic Acids Res 2002; Feb 15;30(4):e15.

73. Kim VN. MicroRNA precursors in motion: exportin-5 mediates their nuclear export. Trends Cell Biol 2004; Apr;14(4):156-9.

74. Lee Y, Ahn C, Han J, Choi H, Kim J, Yim J, Lee J, Provost P, Rådmark O, Kim S, Kim VN. The nuclear RNase III Drosha initiates microRNA processing. Nature 2003; Sep 25;425(6956):415-9.

75. Khanin R, Vinciotti V. Computational modeling of post-transcriptional gene regulation by microRNAs. J Comput Biol 2008; Apr;15(3):305-16.

76. Suarez Y, Fernandez-Hernando C, Pober JS, Sessa WC. Dicer dependent microRNAs regulate gene expression and functions in human endothelial cells. Circ Res 2007; Apr 27;100(8):1164-73.

77. Kim VN. MicroRNA biogenesis: coordinated cropping and dicing. Nat Rev Mol Cell Biol 2005; May;6(5):376-85.

78. Schroeder A, Mueller O, Stocker S, Salowsky R, Leiber M, Gassmann M, Lightfoot S, Menzel W, Granzow M, Ragg T. The RIN: an RNA integrity number for assigning integrity values to RNA measurements. BMC Mol Biol 2006; Jan 31;7:3.

79. Wang H, Ach RA, Curry B. Direct and sensitive miRNA profiling from low-input total RNA. RNA 2007; Jan;13(1):151-9.

80. Li J, Smyth P, Flavin R, Cahill S, Denning K, Aherne S, Guenther SM, O'Leary JJ, Sheils O. Comparison of miRNA expression patterns using total RNA extracted from matched samples of formalin-fixed paraffin-embedded (FFPE) cells and snap frozen cells. BMC Biotechnol 2007; Jun 29;7:36.

81. Nelson PT, Baldwin DA, Scearce LM, Oberholtzer JC, Tobias JW, Mourelatos Z. Microarray-based, high-throughput gene expression profiling of microRNAs. Nat Methods 2004; Nov;1(2):155-61.

82. Loudig O, Milova E, Brandwein-Gensler M, Massimi A, Belbin TJ, Childs G, Singer RH, Rohan T, Prystowsky MB. Molecular restoration of archived transcriptional profiles by complementary-template reverse-transcription (CT-RT). Nucleic Acids Res 2007;35(15):e94.

83. Medeiros F, Rigl CT, Anderson GG, Becker SH, Halling KC. Tissue handling for genome-wide expression analysis: a review of the issues, evidence, and opportunities. Arch Pathol Lab Med 2007; Dec;131(12):1805-16.